Supporting Information

Racemization barriers of atropisomeric 3,3′-bipyrroles: An experimental study with theoretical verification

Sourav Chatterjee,[a] Glenn L. Butterfoss,[b] Madhumita Mandal,[a] Bishwajit Paul,[c] Sreya Gupta,[a] Richard Bonneau,[d] and Parasuraman Jaisankar[a,*]

[a]*Laboratory of Catalysis and Chemical Biology, Department of Organic and Medicinal Chemistry, CSIR-Indian Institute of Chemical Biology, 4 Raja S. C. Mullick Road, Kolkata - 700 032, India.*
[b]*Center for Genomics and Systems Biology, New York University, Abu Dhabi, Abu Dhabi-129188, United Arab Emirates.*
[c]*Brigham and Women's Hospital, Harvard Medical School, Boston, MA - 02115, United States.*
[d]*Center for Genomics and Systems Biology, New York University, New York, United States.*

Email: jaisankar@iicb.res.in

Section I: General Information

All reagents were purchased from commercial suppliers and used without further purification. ^{1}H NMR spectra were recorded on a Bruker DPX 300 MHz or 600 MHz NMR instrument at ambient temperature in CD_3OD or DMSO-d_6. ^{13}C NMR spectra were recorded at 75 MHz or 150 MHz at ambient temperature with TMS as the internal standard. The ^{13}C NMR spectra were recorded with complete proton decoupling. All chemical shifts are reported in ppm. ESI HRMS spectrum was recorded on a Waters® Micromass® Q-TOF micro™ Mass Spectrometer. Analytical thin-layer chromatography (TLC) was carried out on Merck 20 × 20 cm silica gel 60-F_{254} plates. Column chromatography was done with Biotage flash, silica gel 100-200 mesh. HPLC analyses were performed on a Shimadzu SPD-M10AVP using Daicel Chiralcel OJ-H column or Chiralcel OD-H column (5 μm × 4.6 mm × 250 mm). Circular dichroism spectra were recorded on a JASCO J815 unit (Jasco International Co.) equipped with a temperature controller and thermal programmer model PFD 425L/15 in strain free quartz cuvette (55.0 x 10.0 x 2.0 mm internal dimension) having PTFE stopper in "ground type" joint. Quantum calculations were done with Gaussian 09. To identify preliminary minima and barriers, initial conformational scans (data not shown) of the various molecules were done with the axial torsion constrained at 5° increments around 360° and optimized at HF/6-31G* (followed by energy calculations at B3LYP/6-311G** and M05-2X/6-311G**); molecules including ester groups were optimized with various starting orientations of the ester groups for each axial torsion value. Selected geometries were re-optimized at the B3LYP/6-311G** level of theory, followed by single point calculations with the indicated levels of theory and solvent models. Transition states were optimized in stages, with the final optimization using the Opt (TS, NoEigenTest, CalcFC) options. Frequency calculations were conducted on all reported geometries to verify status as a local minimum or transition state and to predict relative free energies. Compounds **1-3** were synthesized by our previous literature procedure; spectral data (^{1}H NMR, ^{13}C NMR and ESI-HRMS) were completely matched.[1]

Section II: Analytical data for compound 1

II.a) Spectral analysis of Electronic Circular Dichroism (ECD)

[1] CD spectra of (*R*)-1 at variable temperatures

To perform the Electronic Circular Dichroism (ECD) analysis, 2.20 mM solution of (*R*)-**1** was prepared by dissolving 1.0 mg of (*R*)-**1** in 1.0 mL EtOH. 400 µL of the above solution was taken in a screw cap quartz cuvette (screw cap is necessary to stop the change of concentration of sample due to solvent evaporation) and placed inside the CD spectrophotometer equipped with thermoelectric temperature controller. CD spectra were obtained from the same sample for each 10 K raise of temperature from 293 to 353 K. The spectral data was obtained is represented below.

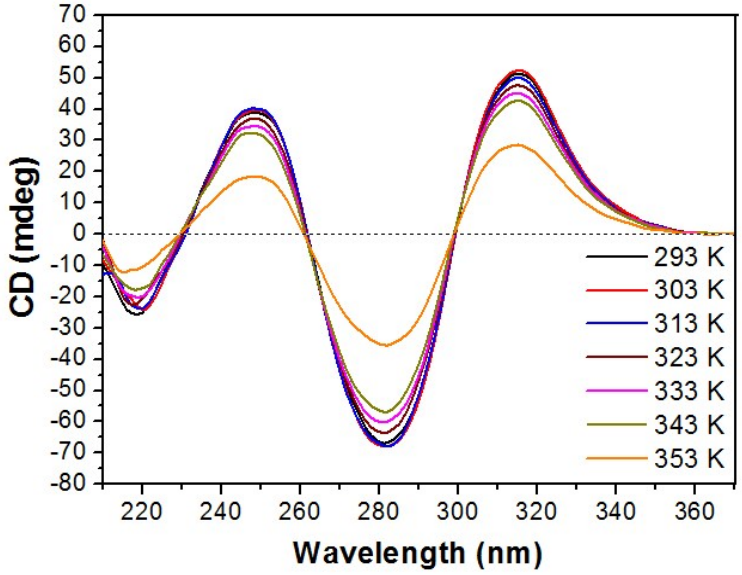

Figure S1: CD spectra of (*R*)-**1** at variable temperatures.

Table S1: CD intensities and calculated enantiomeric excess (*ee*) at variable temperatures.

Temp (K)	293	303	313	323	333	343	353
CD_{max} (mdeg)	52.33	51.25	50.08	47.56	45.12	42.67	28.57
ee (%)[a]	>99.0	96.94	94.74	89.97	85.36	80.73	54.06

[a] Calculated from CD_{max} (mdeg) intensity by unitary method considering 52.33 mdeg value of CD_{max} as >99.0 % *ee* of 2.20 mM enantiopure *(R)*-**1**

[2] CD spectra of (*R*)-1 at 353 K with the course of time

To perform the Electronic Circular Dichroism (ECD) analysis with respect to variable time regime at fixed temperature, 2.20 mM ethanolic solution of (*R*)-**1** was

placed inside the preheated CD spectrophotometer at 353 K. CD spectra were recorded in 20 min time interval up to 160 min.

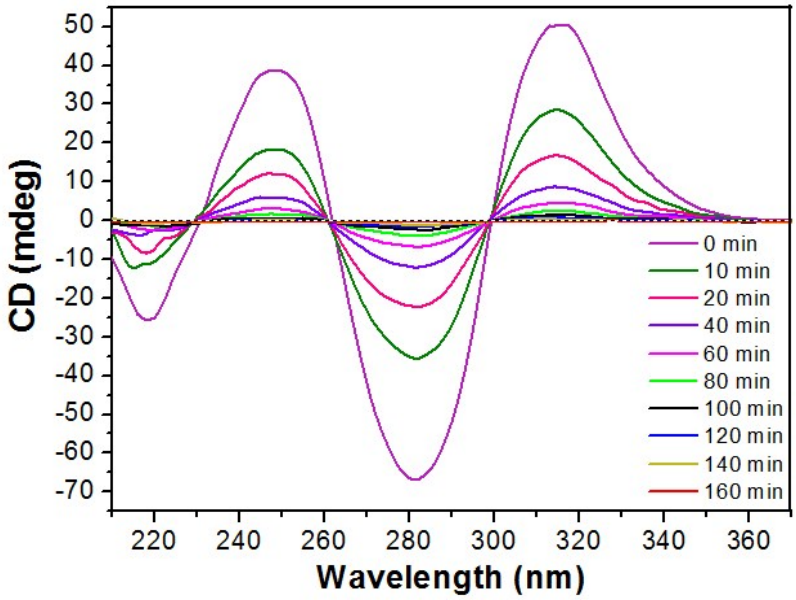

Figure S2: CD spectra of (*R*)-**1** at 353 K in different time scale.

Table S2: CD intensities and calculated enantiomeric excess (*ee*) at 353 K different time scale.

Time (min)	0	10	20	40	60	80	100	120	140	160
CD_{max} (mdeg)	50.56	32.86	20.79	8.75	4.52	2.64	1.47	0.89	0.40	0.03
ee (%)[a]	>99.0	64.35	40.71	17.13	8.85	5.18	2.88	1.75	0.80	0.06

[a] Calculated from CD_{max} (mdeg) intensity by unitary method considering 50.56 mdeg value of CD_{max} as >99.0 % ee of 2.20 mM enantiopure *(R)*-**1**.

[3] CD spectra of (*R*)-1 at 343 K with the course of time

To perform the Electronic Circular Dichroism (ECD) analysis with respect to variable time regime at fixed temperature, 2.20 mM ethanolic solution of (*R*)-**1** was placed inside the preheated CD spectrophotometer at 343 K. CD spectra were recorded in 20 min time interval up to 160 min.

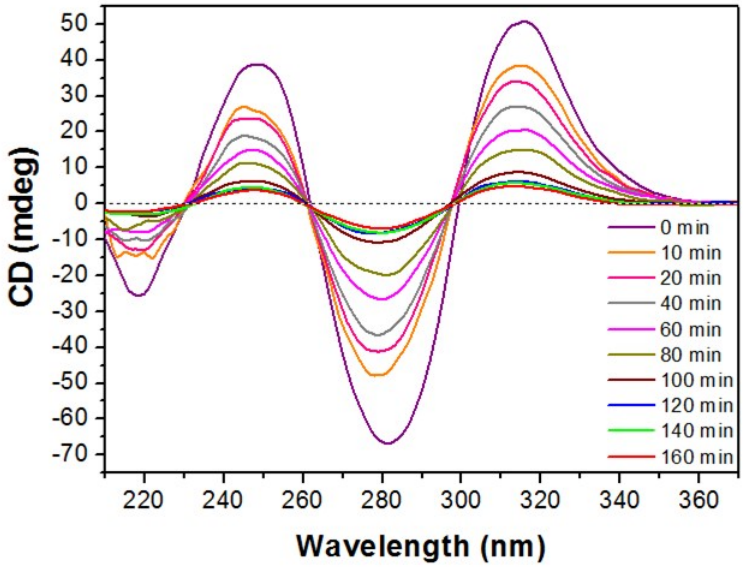

Figure S3: CD spectra of (*R*)-**1** at 343 K in different time scale.

Table S3: CD intensities and calculated enantiomeric excess (*ee*) at 343 K different time scale.

Time (min)	0	10	20	40	60	80	100	120	140	160
CD_{max} (mdeg)	50.79	38.50	34.14	27.07	20.67	14.89	8.79	6.14	5.82	4.83
ee(%)[a]	>99.0	75.04	66.54	52.76	40.29	29.02	17.13	11.96	11.34	9.41

[a] Calculated from CD_{max} (mdeg) intensity by unitary method considering 50.79 mdeg value of CD_{max} as >99.0 % ee of 2.20 mM enantiopure *(R)*-**1**.

[4] CD spectra of (*R*)-1 at 333 K with time

To perform the Electronic Circular Dichroism (ECD) analysis with respect to variable time regime at fixed temperature, 2.20 mM ethanolic solution of (*R*)-**1** was placed inside the preheated CD spectrophotometer at 333 K. CD spectra were recorded in 20 min time interval up to 160 min.

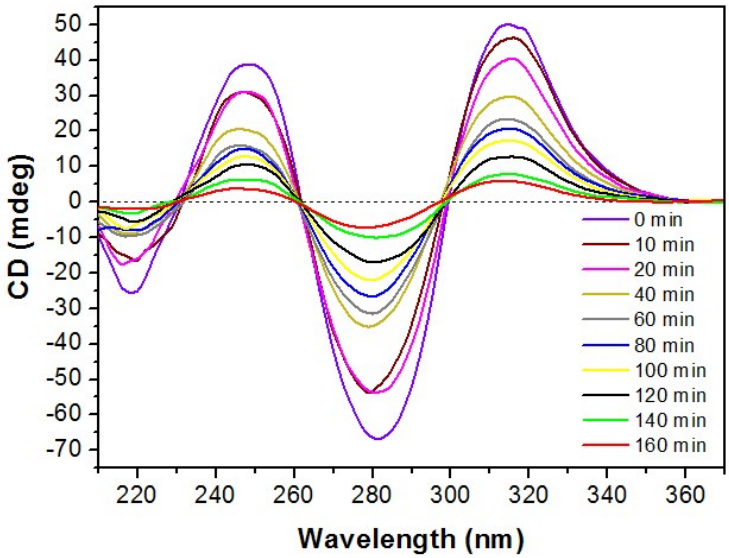

Figure S4: CD spectra of (*R*)-**1** at 333 K in different time scale.

Table S4: CD intensities and calculated enantiomeric excess (*ee*) at 333 K different time scale

Time (min)	0	10	20	40	60	80	100	120	140	160
CD_{max} (mdeg)	50.0	46.26	40.45	29.69	23.38	20.78	17.45	12.76	7.79	5.93
ee (%)[a]	>99.0	91.59	80.09	58.78	46.29	41.14	34.55	25.26	15.42	11.74

[a] Calculated from CD_{max} (mdeg) intensity by unitary method considering 50.0 mdeg value of CD_{max} as >99.0 % ee of 2.20 mM enantiopure *(R)*-**1**.

II.b) Determination of kinetic and thermodynamical parameters from ECD analysis[2]

CD intensities (mdeg) of (*R*)-**1** as a function of time (min) were plotted at different temperatures (333, 343, and 353 K in figure S5). The decay constants (t_1), rate constants (k_{rac}), and equilibrium constants ($K^{\neq}_{eq}$) for the racemisation were determined from the exponential decay curves for each of the temperatures by using the following equations Eqn.1, 2, and 3 respectively.

Eqn. 1: $y = A1 * \exp(-\frac{x}{t_1}) + y_0$ (where, A1 = amplitude, t_1 = decay constant and y_0 = offset)

Eqn. 2: $k_{rac} = \frac{1}{t_1}$ (k_{rac} = racemization rate constant)

Eqn. 3: $K^{\neq}_{eq} = \frac{hk_{rac}}{\kappa T k_B}$ (where h = Planck constant, κ = transmission coefficient, T = temperature and k_B = Boltzmann constant)

The energy ($\Delta G^{\neq}_{rac}$) barrier for racemisation was further calculated using the following Eyring equation (Eqn. 4).

Eqn. 4: $\Delta G^{\neq}_{rac} = -RT\ln(\frac{hk_{rac}}{\kappa T k_B}) = -RT\ln K^{\neq}_{eq}$

The activation enthalpy ($\Delta H^{\neq}_{rac}$) and activation entropy ($\Delta S^{\neq}_{rac}$) of the isomerization of atropisomer **1** were further determined employing the Eyring equation (Eqn 5) (see: Section II.e for details).

Eqn. 5: $\ln\frac{k_{rac}}{T} = -\frac{\Delta H^{\neq}_{rac}}{R}\frac{1}{T} + \ln\frac{k_B}{h} + \frac{\Delta S^{\neq}_{rac}}{R}$

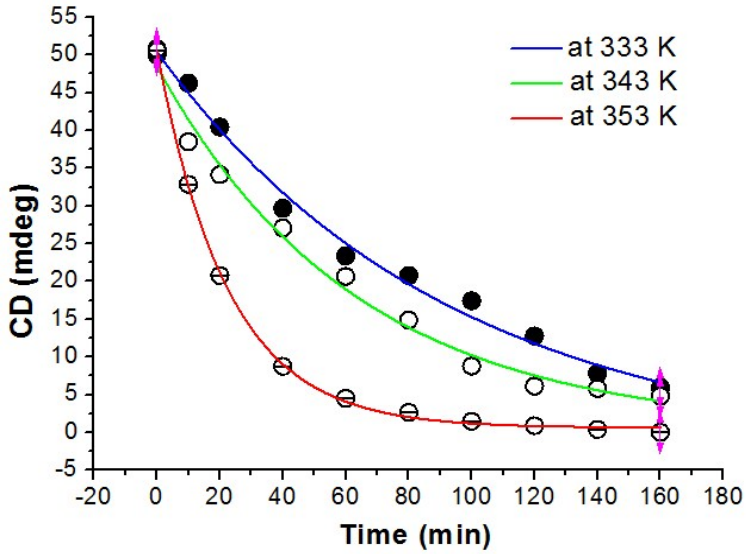

Figure S5: Plot of CD (mdeg) of (*R*)-**1** as a function of time (min)

II.c) HPLC profiles at different time intervals at 353 K

1.0 mg of (*R*)-**1** was isolated through chiral HPLC and dissolved in 1.0 mL of ethanol to prepare 2.20 mM ethanolic solution. The mother solution was fractionated in ten parts and each of 100 µL solution of (*R*)-**1** was transferred into ten closed cap glass vials which were kept inside a preheated incubator at 353 K. Each sample was taken out from the incubator at a time interval of 20 min and stored at 273 K (to immediately stop the further racemisation process). Individual samples were then straight away subjected to chiral HPLC analysis by using following condition:

Column: Chiral CEL OJ-H (4.6 mm x 250.0 mm x 5.0 µm)

Solvent: 0.30 % diethyl amine in hexane : ethanol (90 : 10)

Flow rate: 1.0 mL/min

Mode: Binary gradient

Column oven: 298 K

Injected volume: 40.0 µL

It was observed that bipyrroles undergo slow aerial oxidation over the time during HPLC analysis resulted in smaller decomposed products in the range of 3-9 min. which could not be prevented in the optimized HPLC condition.[3]

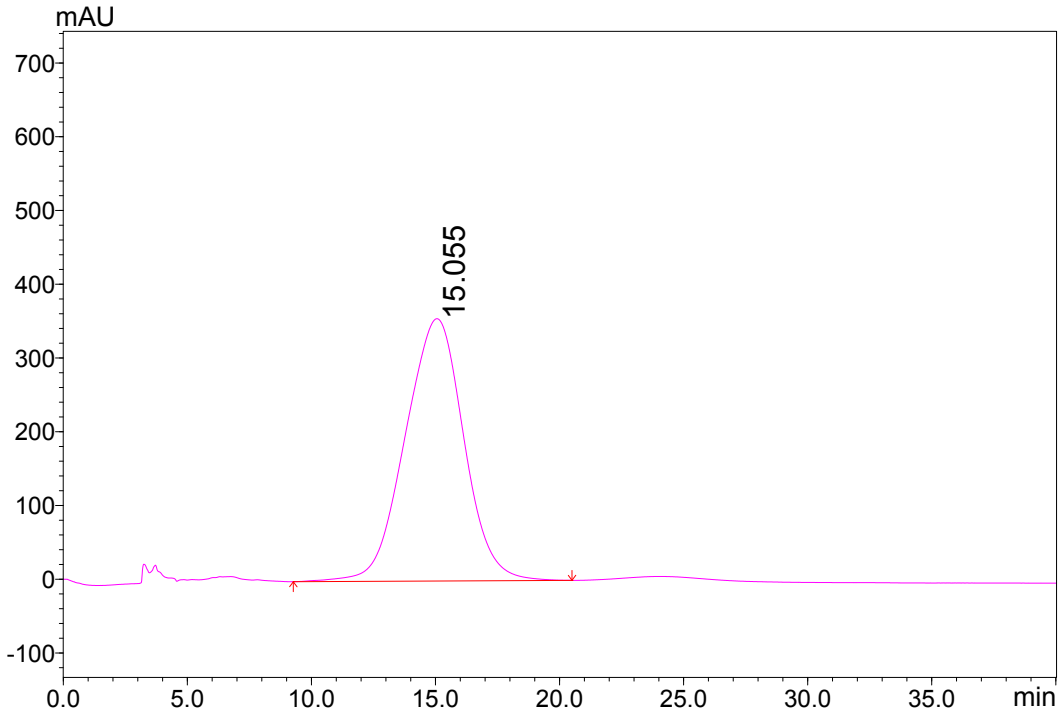

PDA Ch1 265nm 4nm

Peak#	Ret. Time	Area	Height	Area %	Height %
1	15.055	58460410	355710	100.000	100.000
Total		58460410	355710	100.000	100.000

Figure S6: Chiral HPLC profile of (*R*)-**1** at 0 min (before placing incubation at 353 K)

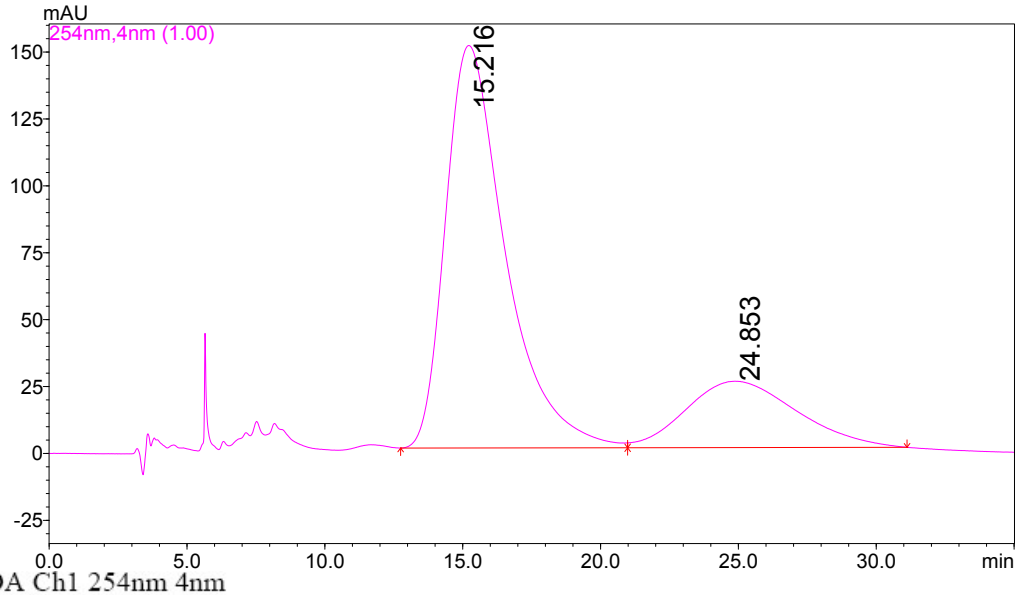

PDA Ch1 254nm 4nm

Peak#	Ret. Time	Area	Height	Area %	Height %
1	15.216	22749514	150430	76.622	85.845
2	24.853	6940902	24805	23.378	14.155
Total		29690416	175235	100.000	100.000

Figure S7: Chiral HPLC profile of (*R*)-**1** at 20 min (353 K)

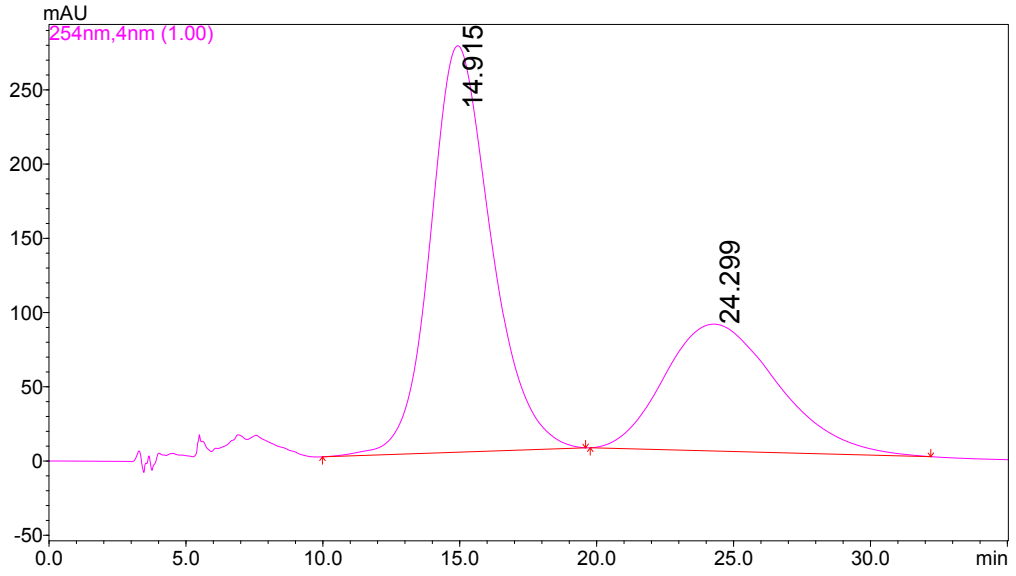

PDA Ch1 254nm 4nm

Peak#	Ret. Time	Area	Height	Area %	Height %
1	14.915	42395046	273699	63.286	76.200
2	24.299	24594918	85487	36.714	23.800
Total		66989964	359185	100.000	100.000

Figure S8: Chiral HPLC profile of (*R*)-**1** at 40 min (353 K)

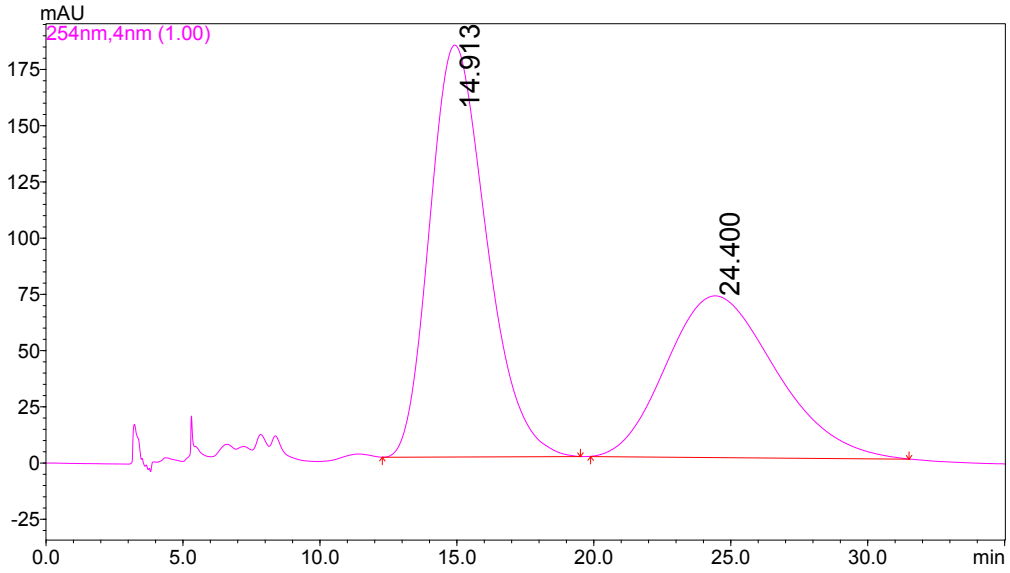

PDA Ch1 254nm 4nm

Peak#	Ret. Time	Area	Height	Area %	Height %
1	14.913	26457324	183154	56.900	71.805
2	24.400	20040386	71917	43.100	28.195
Total		46497709	255070	100.000	100.000

Figure S9: Chiral HPLC profile of (*R*)-**1** at 60 min (353 K)

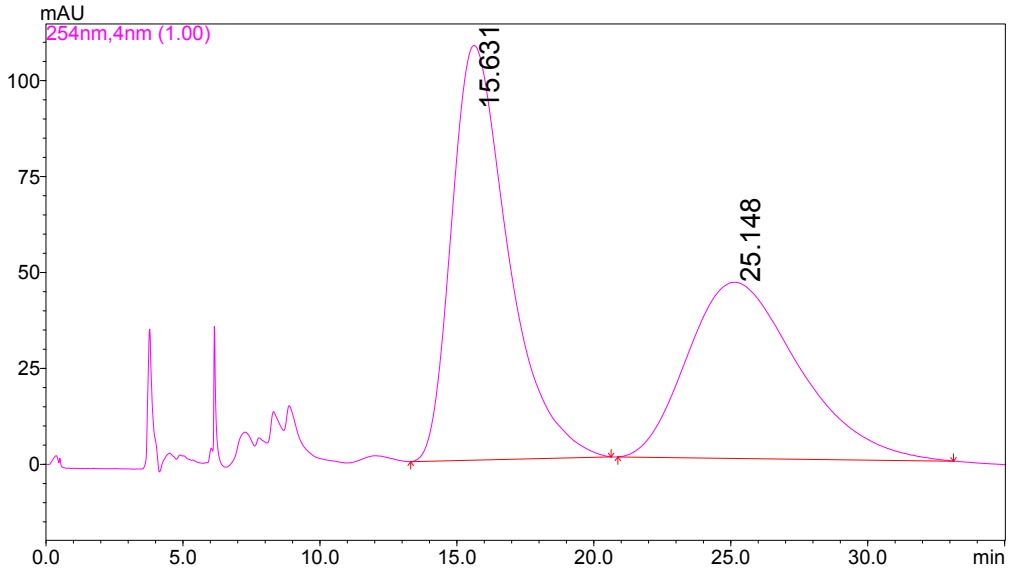

PDA Ch1 254nm 4nm

Peak#	Ret. Time	Area	Height	Area %	Height %
1	15.631	15558006	108116	54.504	70.184
2	25.148	12986828	45930	45.496	29.816
Total		28544834	154046	100.000	100.000

Figure S10: Chiral HPLC profile of (*R*)-**1** at 80 min (353 K)

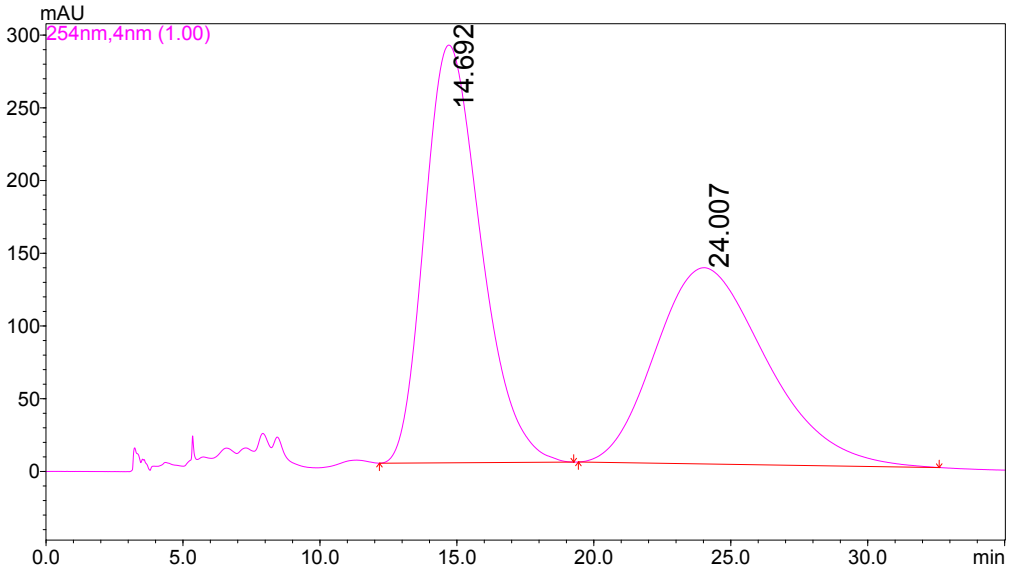

PDA Ch1 254nm 4nm

Peak#	Ret. Time	Area	Height	Area %	Height %
1	14.692	41120588	287165	51.878	68.038
2	24.007	38143517	134903	48.122	31.962
Total		79264105	422068	100.000	100.000

Figure S11: Chiral HPLC profile of (*R*)-**1** at 100 min (353 K)

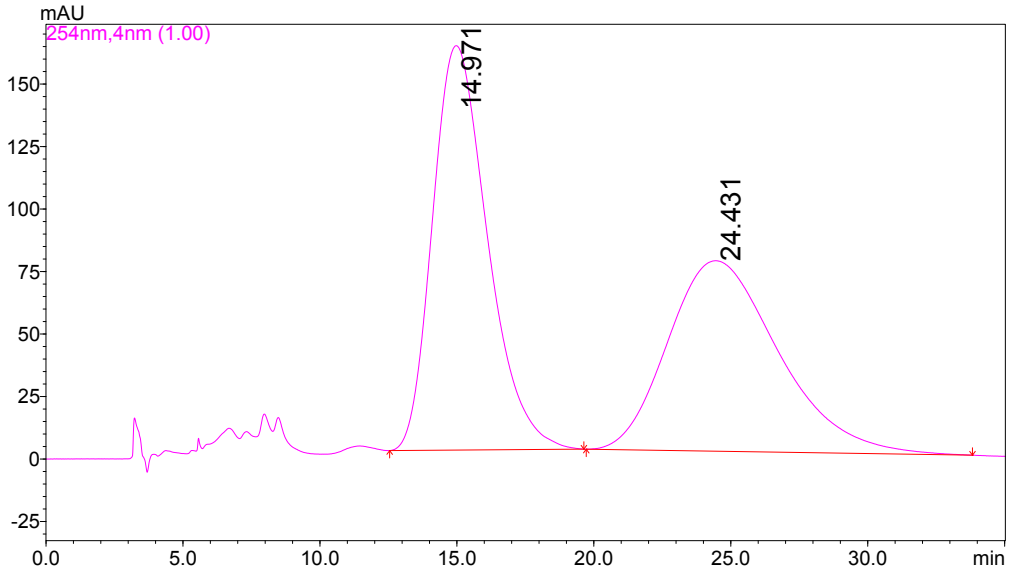

PDA Ch1 254nm 4nm

Peak#	Ret. Time	Area	Height	Area %	Height %
1	14.971	22597969	161787	51.378	67.981
2	24.431	21385722	76203	48.622	32.019
Total		43983691	237990	100.000	100.000

Figure S12: Chiral HPLC profile of (*R*)-**1** at 120 min (353 K)

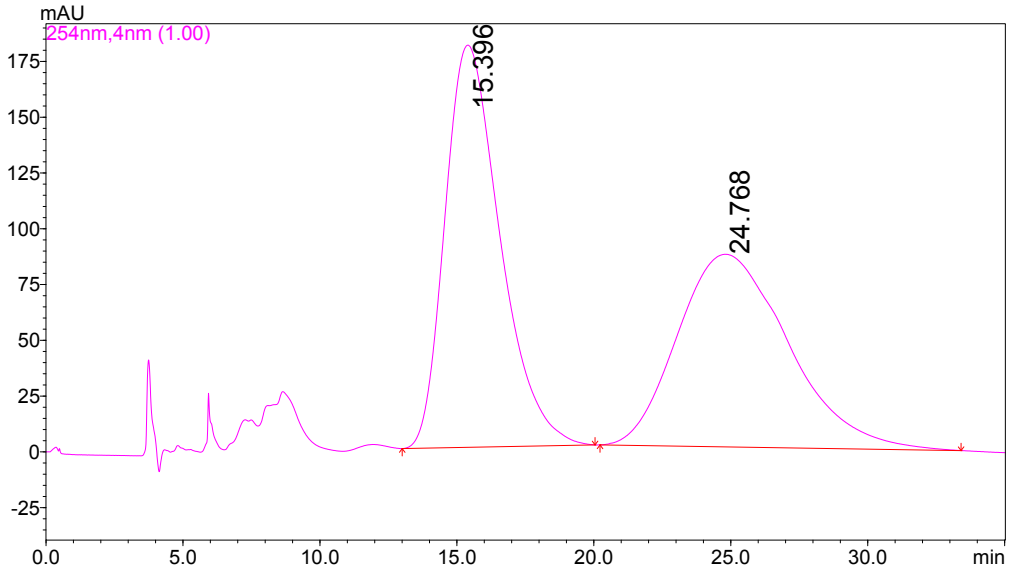

PDA Ch1 254nm 4nm

Peak#	Ret. Time	Area	Height	Area %	Height %
1	15.396	25262056	180269	50.936	67.618
2	24.768	24333885	86330	49.064	32.382
Total		49595941	266600	100.000	100.000

Figure S13: Chiral HPLC profile of (*R*)-**1** at 140 min (353 K)

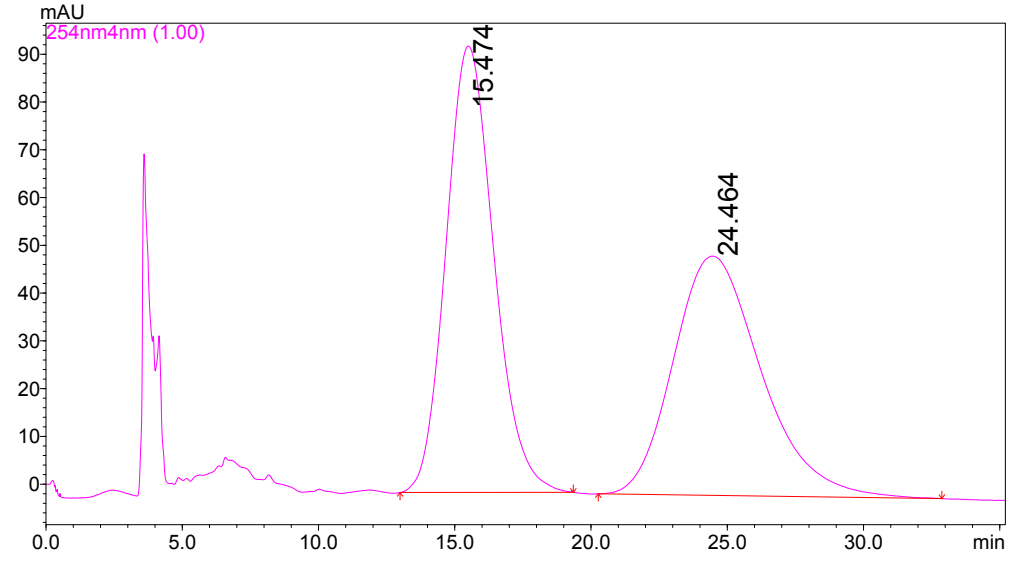

PDA Ch2 254nm 4nm

Peak#	Ret. Time	Area	Height	Area %	Height %
1	15.474	11406629	93434	50.372	65.092
2	24.464	11237975	50107	49.628	34.908
Total		22644604	143541	100.000	100.000

Figure S14: Chiral HPLC profile of (*R*)-**1** at 160 min (353 K)

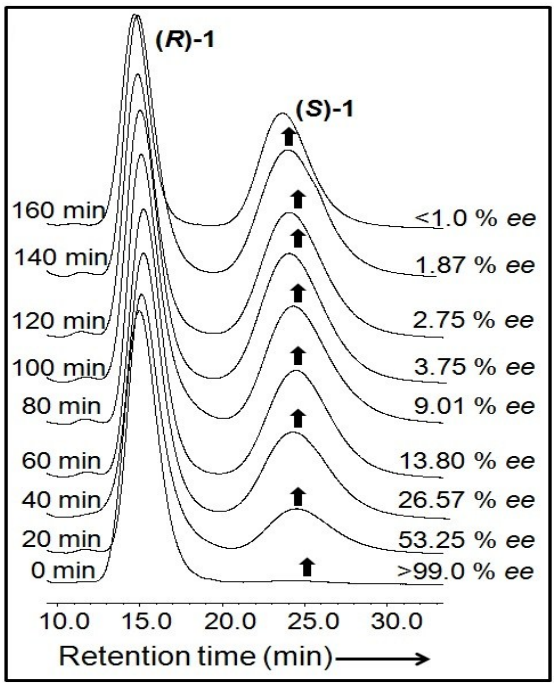

Figure S15: Chiral HPLC profiles for time dependent racemization of **1** at 353 K.

II.d) HPLC profiles at different time intervals at 300 K

Same experimental method was employed as in **Section II.c**.

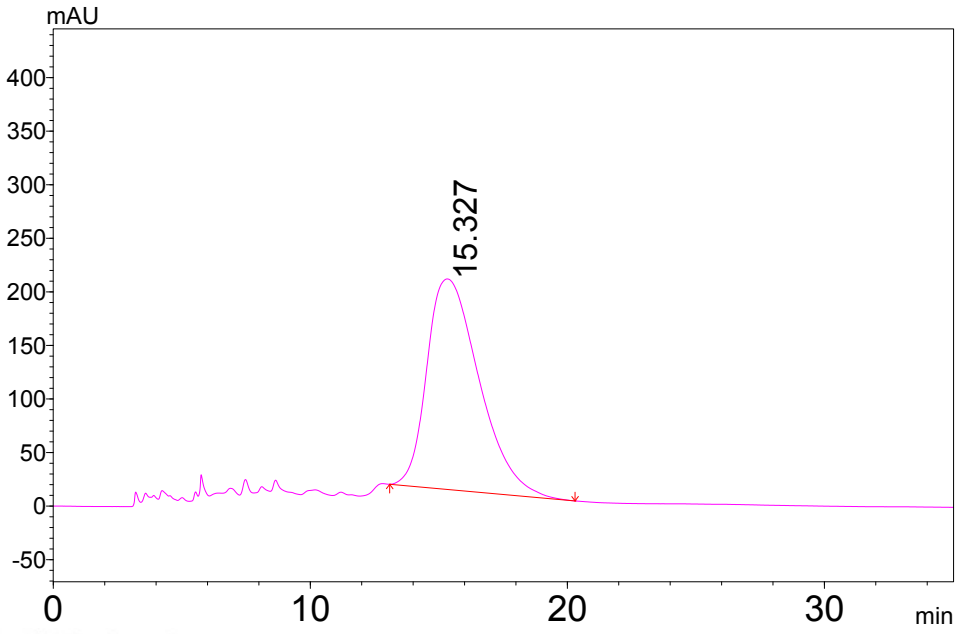

PDA Ch1 254nm 4nm

Peak#	Ret. Time	Area	Height	Area %	Height %
1	15.327	27859314	196488	100.000	100.000
Total		27859314	196488	100.000	100.000

Figure S16: Chiral HPLC profile of (*R*)-**1** at 0 day (before placing incubation at 300 K)

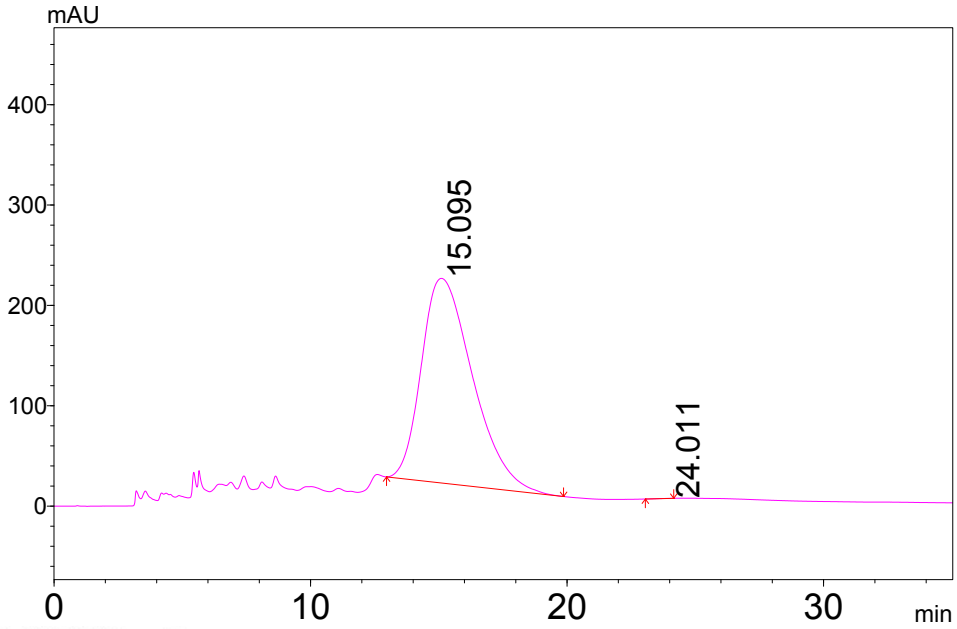

PDA Ch1 254nm 4nm

Peak#	Ret. Time	Area	Height	Area %	Height %
1	15.095	28425827	203853	99.991	99.985
2	24.011	2436	31	0.009	0.015
Total		28428264	203884	100.000	100.000

Figure S17: Chiral HPLC profile of (*R*)-**1** at 1 day (300 K)

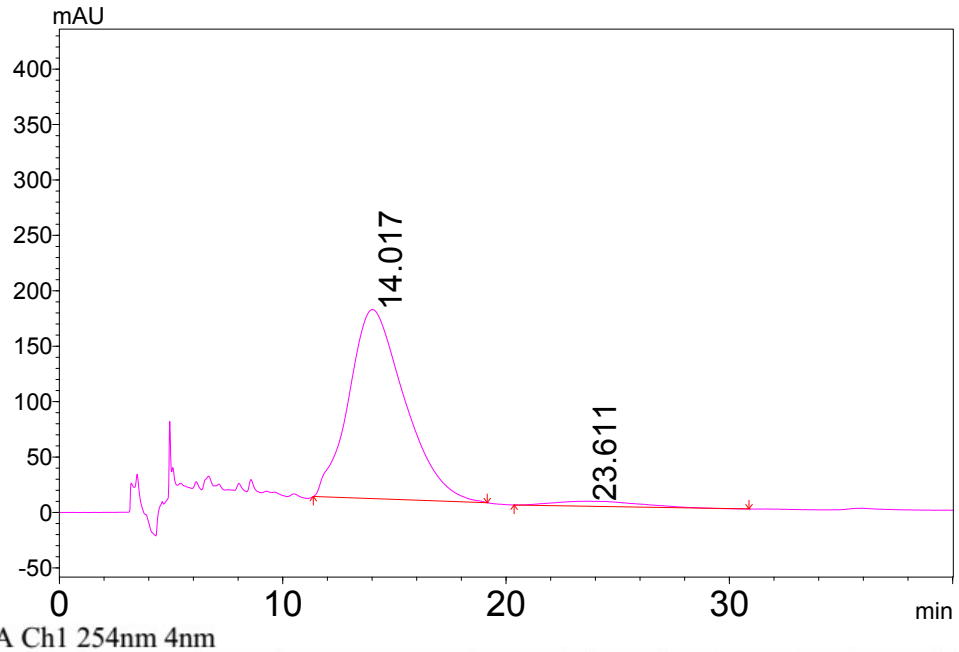

PDA Ch1 254nm 4nm

Peak#	Ret. Time	Area	Height	Area %	Height %
1	14.017	29694775	170547	96.119	97.421
2	23.611	1199080	4514	3.881	2.579
Total		30893855	175061	100.000	100.000

Figure S18: Chiral HPLC profile of (*R*)-**1** at 2 days (300 K)

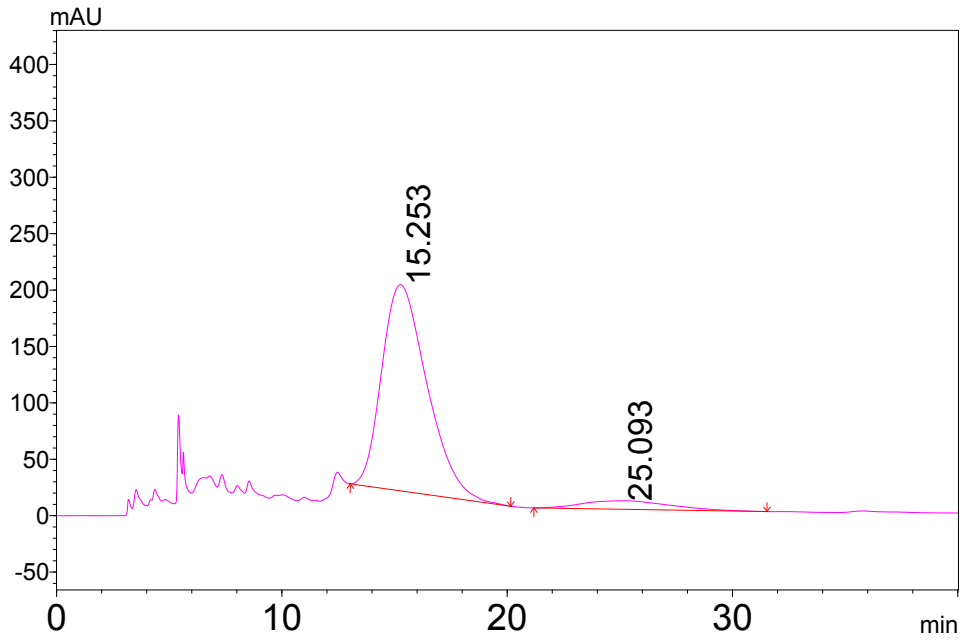

PDA Ch1 254nm 4nm

Peak#	Ret. Time	Area	Height	Area %	Height %
1	15.253	25540025	182777	92.555	96.017
2	25.093	2054441	7583	7.445	3.983
Total		27594466	190360	100.000	100.000

Figure S19: Chiral HPLC profile of (*R*)-**1** at 3 days (300 K)

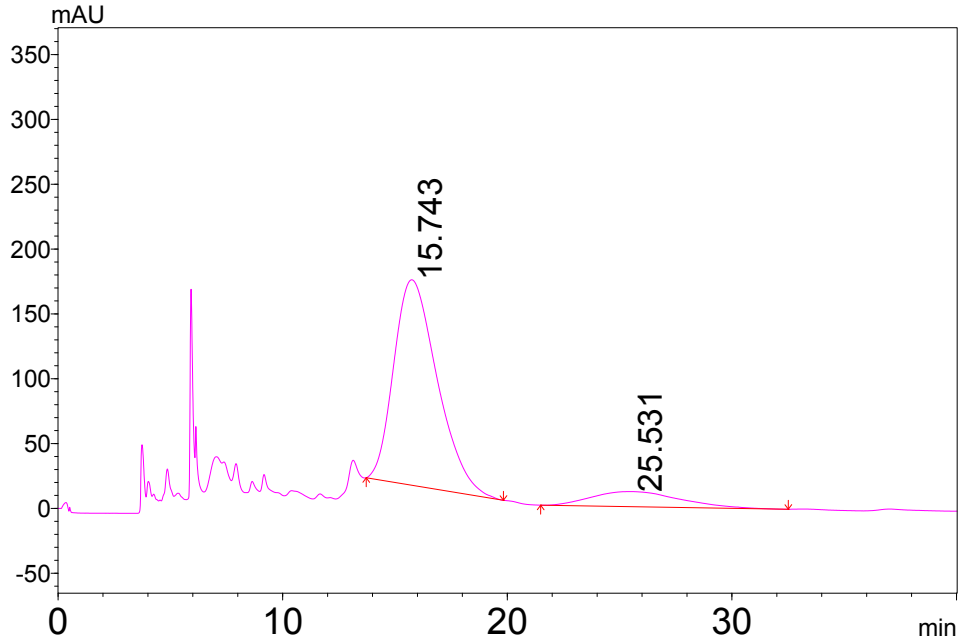

PDA Ch1 254nm 4nm

Peak#	Ret. Time	Area	Height	Area %	Height %
1	15.743	21383204	158435	87.040	93.160
2	25.531	3183891	11633	12.960	6.840
Total		24567095	170068	100.000	100.000

Figure S20: Chiral HPLC profile of (*R*)-**1** at 5 days (300 K)

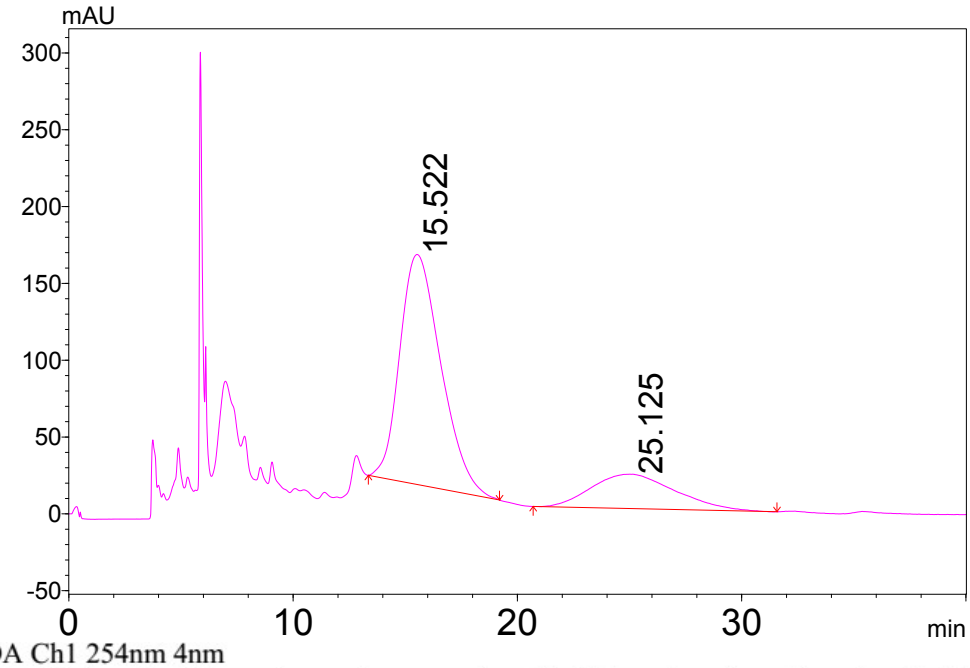

PDA Ch1 254nm 4nm

Peak#	Ret. Time	Area	Height	Area %	Height %
1	15.522	19122946	149695	76.776	86.983
2	25.125	5784530	22402	23.224	13.017
Total		24907476	172096	100.000	100.000

Figure S21: Chiral HPLC profile of (*R*)-**1** at 10 days (300 K)

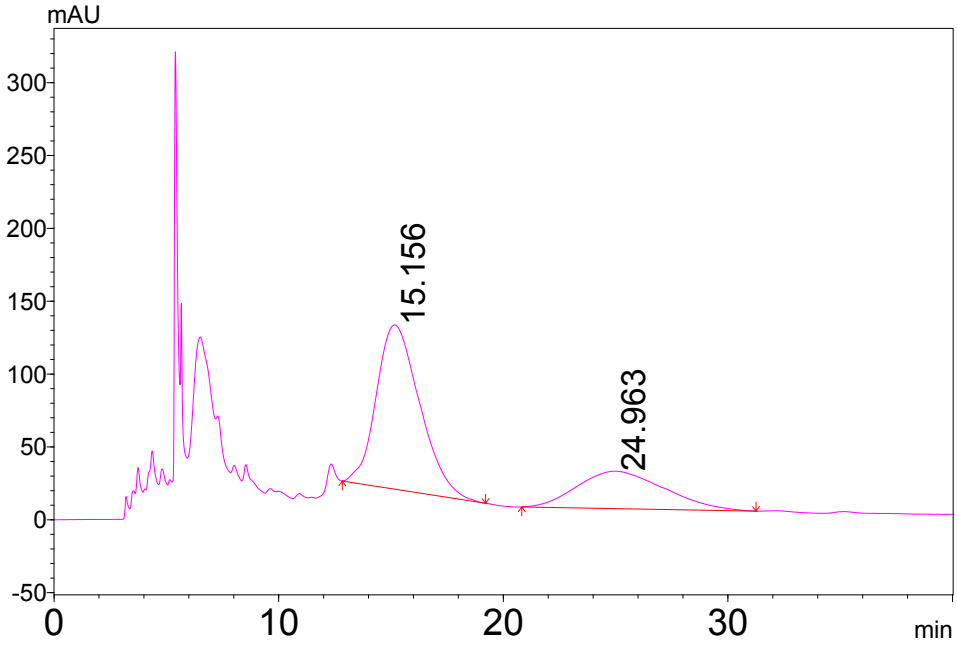

PDA Ch1 254nm 4nm

Peak#	Ret. Time	Area	Height	Area %	Height %
1	15.156	15204955	112710	68.696	81.415
2	24.963	6928813	25729	31.304	18.585
Total		22133768	138439	100.000	100.000

Figure S22: Chiral HPLC profile of (*R*)-**1** at 15 days (300 K)

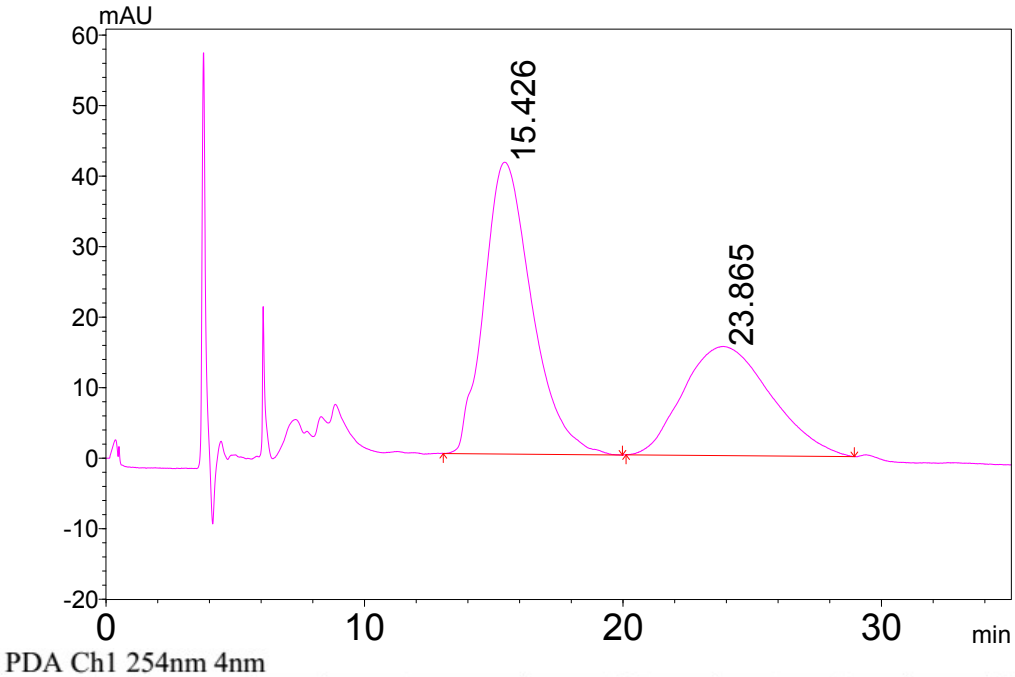

PDA Ch1 254nm 4nm

Peak#	Ret. Time	Area	Height	Area %	Height %
1	15.426	5320838	41378	59.289	72.760
2	23.865	3653572	15491	40.711	27.240
Total		8974410	56869	100.000	100.000

Figure S23: Chiral HPLC profile of (*R*)-**1** at 20 days (300 K)

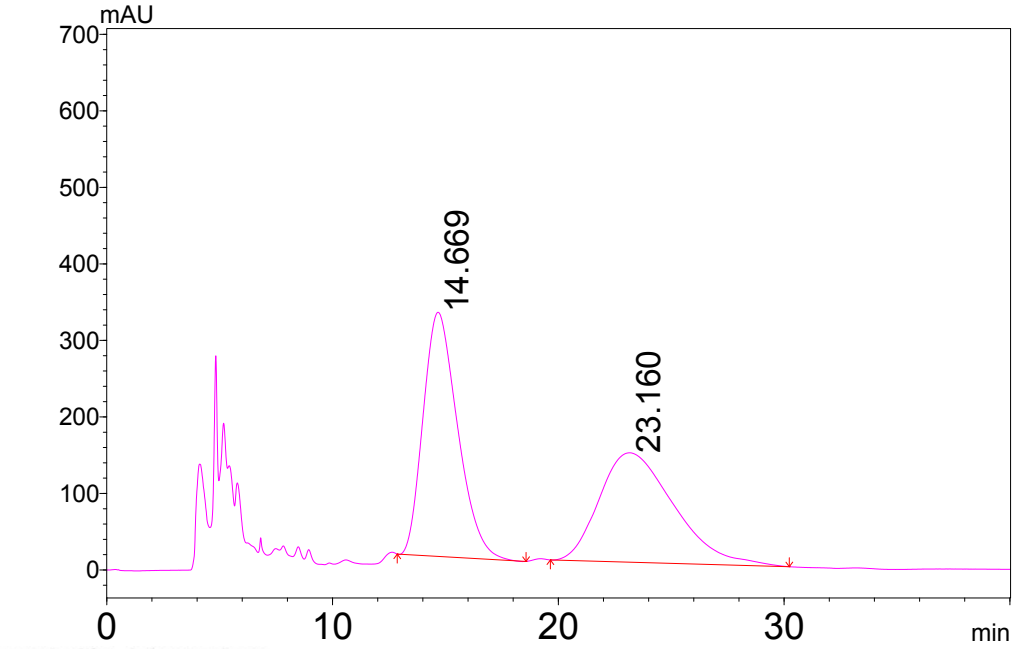

PDA Ch1 265nm 4nm

Peak#	Ret. Time	Area	Height	Area %	Height %
1	14.669	33886720	319110	50.823	69.055
2	23.160	32789163	142998	49.177	30.945
Total		66675883	462108	100.000	100.000

Figure S24: Chiral HPLC profile of (*R*)-**1** at 25 days (300 K)

II.e) Verification of kinetic and thermodynamical parameters by HPLC analysis[4]

In order to verify the racemisation energy and other kinetic and thermodynamical parameters obtained from ECD analysis, time dependent chiral HPLC analysis was performed on enantiopure (*R*)-**1** following the experimental protocol mentioned in **section II.c**. The decrease of enantiomeric excess (*ee*) with time at 353 K and 300 K incubation temperature are shown in figure S25 and S26 and summarized in table S5 and S6 respectively. Decrease of enantiopurity (*ee* %) of (*R*)-**1** at both the experimental temperatures (353 and 300 K) were plotted as a function of variable time regime. From the exponential decay curve (shown in figure S25 and S26), energy to racemisation and other parameters were determined from equations 1-5 described in **section II.b**. The results obtained from HPLC are in well agreement with the ECD analysis performed at different temperatures.

Table S5: Decrease of enantiomeric excess (*ee* %) with time during incubation of (*R*)-**1** at 353 K.

Time (min)	0	20	40	60	80	100	120	140	160
ee (%)	>99.0	53.25	26.57	13.80	9.01	3.75	2.75	1.87	0.30

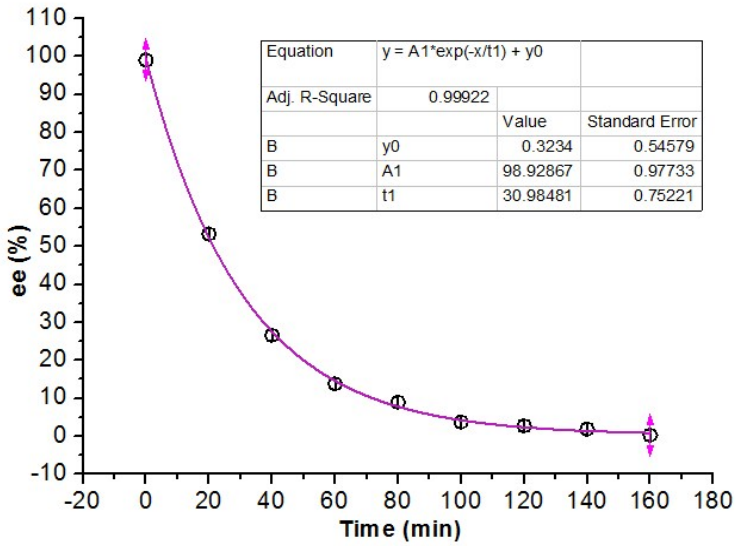

Figure S25: Plot of *ee* (%) of (*R*)-bipyrrole (**1**) as a function of time (min.) at 353 K for the determination of its conformational stability by chiral HPLC.
Regression value of first order decay = 0.9992.

Table S6: Decrease of enantiomeric excess (*ee* %) with time during incubation of (*R*)-**1** at 300 K.

Time (days)	0	1	2	3	5	10	15	20	25
ee (%)	>99.0	99.98	92.0	85.11	74.08	53.55	37.39	18.57	1.65

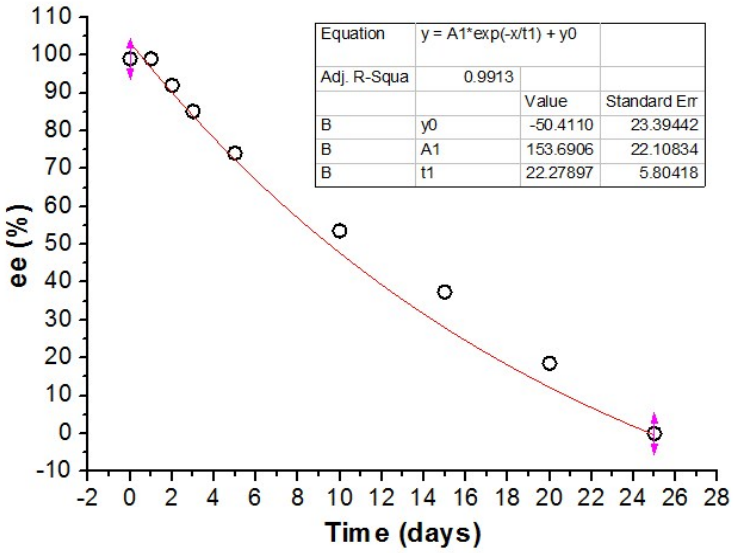

Figure S26: Plot of *ee* (%) of (*R*)-bipyrrole (**1**) as a function of time (min.) at 300 K for the determination of its conformational stability by chiral HPLC.
Regression value of first order decay = 0.9913.

Determination of activation enthalpy ($\Delta H^{\neq}_{rac}$) and activation entropy ($\Delta S^{\neq}_{rac}$) of racemization:

The activation enthalpy ($\Delta H^{\neq}_{rac}$) and activation entropy ($\Delta S^{\neq}_{rac}$) of the isomerization of atropisomer **1** were further determined employing the Eyring equation (Eqn 5):

Eqn. 5: $$\ln\frac{k_{rac}}{T} = -\frac{\Delta H^{\neq}_{rac}}{R}\frac{1}{T} + \ln\frac{k_B}{h} + \frac{\Delta S^{\neq}_{rac}}{R}$$

The values for $\Delta H^{\neq}_{rac}$ and $\Delta S^{\neq}_{rac}$ were determined from kinetic data obtained from a $\ln\frac{k_{rac}}{T}$ vs. $\frac{1}{T}$ plot considering temperature (T) as 333, 343 and 353 K (based on ECD results) as well as 300 K and 353 K (based on HPLC results).[2c] The equation is a straight line with negative slope, $-\frac{\Delta H^{\neq}_{rac}}{R}$, and a y-intercept, $\ln\frac{k_B}{h} + \frac{\Delta S^{\neq}_{rac}}{R}$. The activation enthalpy ($\Delta H^{\neq}_{rac}$) and activation entropy ($\Delta S^{\neq}_{rac}$) of the racemization process were determined as 27.49 kcal.mol^{-1} and 4.92 cal.mol^{-1}.K^{-1} respectively.

II.f) Computationally evaluated additional results

Images of 5,5′-dimethyl-2,2′-diphenyl-1*H*,1′*H*-[3,3′]bipyrrolyl-4,4′-dicarboxylic acid diethyl ester (**1**) ground state and both transition state structures (TS), as predicted at the B3LYP/6-311G**//B3LYP/6-311G** level of theory are shown below (figure S27). Energies are given in table S7, including energies with implicit solvent models, the M05-2X functional, and the estimated free energies via vibrational frequency calculations. The latter should be taken with caution as estimates of entropy, given the harmonic approximations and given only pair of structures is considered to represent the ensemble. (See below for calculation details). The corresponding relative $\Delta H^{\neq}_{rac}$ values are 25.18 kcal.mol^{-1} for TS-I and 27.3 kcal.mol^{-1} for TS-II.

The *syn* TS (**TS1** below) is slightly lower in energy (26.2 kcal.mol^{-1} B3LYP) across the various methods than the *anti* (**TS2**, 28.3 kcal.mol^{-1} B3LYP), although the difference is only 1-3 kcal.mol^{-1} suggesting that at temperature, transitions will not exclusively follow a single pathway. Polar solvent is predicted to have little influence on the barrier height.

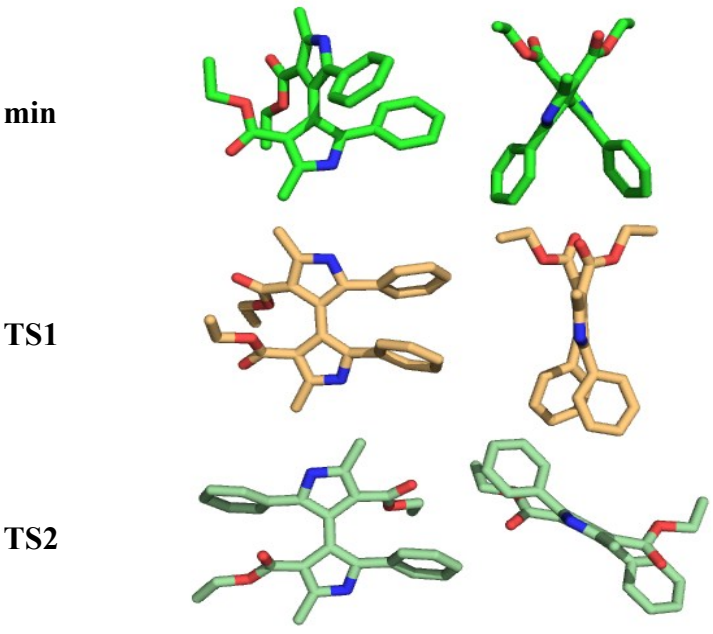

Figure S27: Two views each of the predicted molecule **1** ground states (green) and both the *syn* and *anti* transition states (light orange and pale green).

The rotation barrier of molecule **1** can be more finely analyzed if it is broken down into component interactions. We examined the rotation barriers of several variants of **1** (shown below) possessing different substitution patterns (figure S28, table S7).

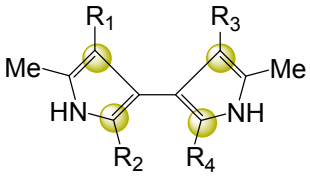

Table S7: Representative molecules for DFT analysis[a]

Molecule	R_1	R_2	R_3	R_4
1a	H	H	H	H
1b	H	Ph	H	Ph
1c	CO_2Me	H	H	Ph
1d	CO_2Me	H	CO_2Me	H
1	CO_2Et	Ph	CO_2Et	Ph

[a] Schematic of the molecules discussed below. The measured axial torsion (from the 2 carbon to the 2´carbon) is highlighted.

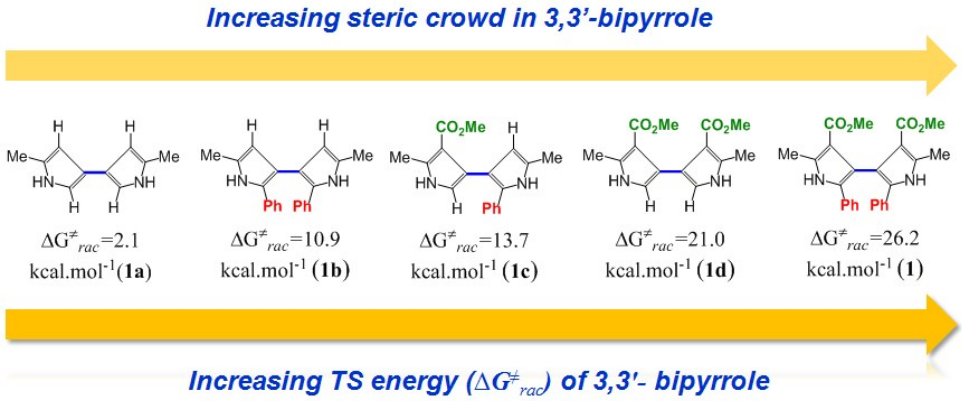

Figure S28: Racemization energy (kcal.mol^{-1}) with sequential increase in steric bulk of 3,3´-bipyrrole system

Table S8: Predicted axial torsions (in degrees) and relative energies under various models (in kcal.mol^{-1}) of optimized and transition state structures for 5,5′-dimethyl-2,2′-diphenyl-1*H*,1′*H*-[3,3′]bipyrrolyl-4,4′-dicarboxylic acid diethyl ester (**1**) and variations thereof.

Molecule	Conformation	Angle	B3LYP[a]	B3LYP[b] (Water)	B3LYP[c] (EtOH)	M05-2X[d]	B3LYP[e] ($\Delta G^{\neq}_{rac}$)
1	min	-64.4	0.0	0.0	0.0	0.0	0.0
	TS1	-4.7	26.2	26.9	26.9	22.0	29.8
	TS2	179.2	28.3	27.6	27.6	25.0	31.4
1a	min	155.0	0.0	0.0	-	0.0	0.0
	TS	92.6	2.1	2.7	-	1.9	3.1
1b	min	160.0	0.0	0.0	-	0.0	0.0
	TS	-18.7	10.9	11.3	-	8.1	12.3
1c	min	119.9	0.0	0.0	-	0.0	0.0
	TS	-171	13.7	13.2	-	12.9	14.1
1d	min	57.6	0.0	0.0	-	0.0	0.0
	TS	-15.6	21.0	19.2	-	18.5	24.4

[a] B3LYP/6-311G**// B3LYP/6-311G**
[b] As above with Polarizable Continuum Model solvent water in energy calculation
[c] As above with Polarizable Continuum Model solvent ethanol in energy calculation
[d] M05-2X/6-311G**// B3LYP/6-311G**
[e] *in vacuo* B3LYP energy with Gibbs free energy $\Delta G^{\neq}_{rac}$) correction from vibrational frequencies (1 atm, 298.15 K)

Analysis of 5,5′-dimethyl-2,2′-diphenyl-1*H*,1′*H*-[3,3′]bipyrrolyl-4,4′-dicarboxylic acid diethyl ester (1) variants

3-(1*H*-pyrrol-3-yl)-1*H*-pyrrole (1a):

The unsubstituted bipyrrole **1a** prefers a slightly off-planar conformation with a minimum axial torsion of 160° (as measured from the 2 carbon to the 2′carbon). This geometry may be due the competing effects of retaining some resonance between the heterocycles and alleviating clashes between the hydrogens. In the predicted TS state, the two rings are nearly perpendicular (92.6°). However, the barrier is quite low,

with TS energies of 1.85 and 2.1 kcal.mol^{-1} given by M05-2X and B3LYP respectively (see table S8).

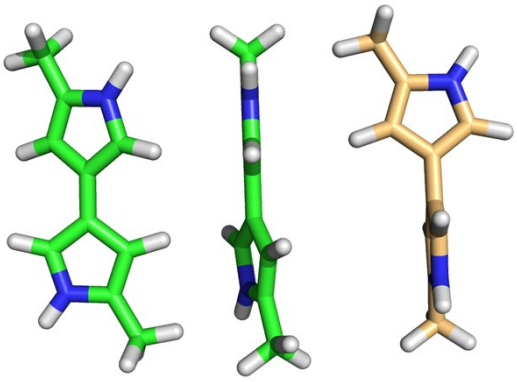

Figure S29: Two views of the **1a** predicted ground state (green) and the TS (light orange).

2-phenyl-3-(2-phenyl-1*H*-pyrrol-3-yl)-1*H*-pyrrole (1b):

The barrier presented by the phenyl rings passing each other can be modeled with **1b**, a 2,2′ phenyl substitution. The minimum energy conformations are further away from planarity relative to **1a**. The overall lowest energy structure has an axial torsion of 137°. The TS for phenyl rings passing each other are at -18.7° is in the range of 10 kcal.mol^{-1}, substantially higher than that of molecule **1**. However, still well below the threshold required for atropisomerism.

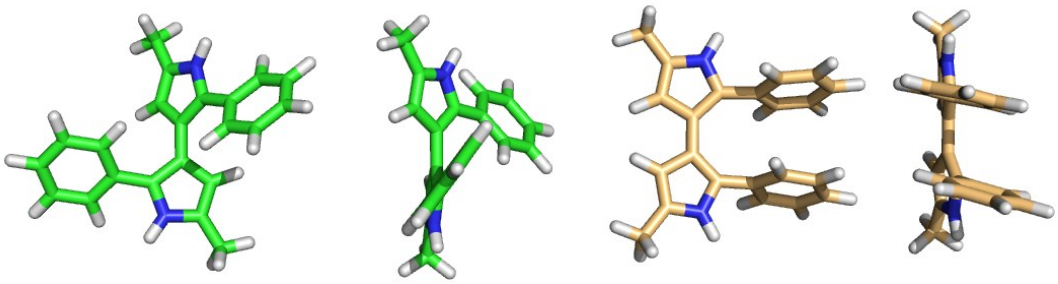

Figure S30: Two views of the **1b** predicted ground state (green) and two views of the TS (light orange).

methyl 2'-phenyl-1H,1'H-[3,3'-bipyrrole]-4-carboxylate (1c):

The transition state energy for the phenyl group passing the ester (molecule **1c**) is predicted to be ~13 kcal.mol^{-1} by both M05-2X and B3LYP. The optimized structure has an axial torsion of 119°.

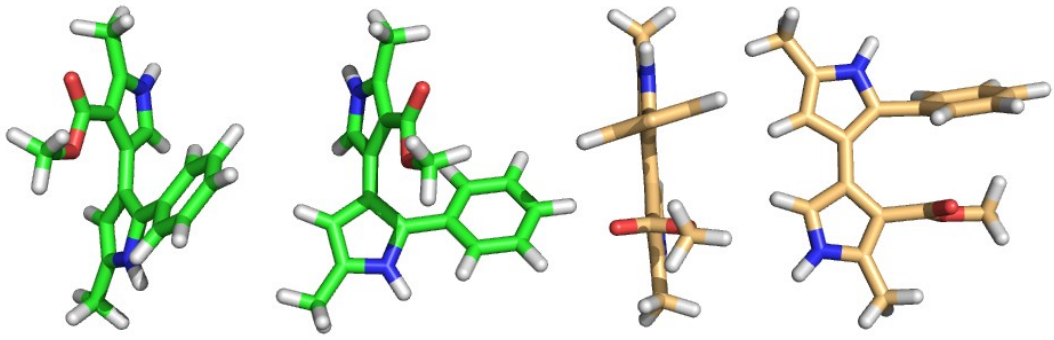

Figure S31: Two views of the **1c** predicted ground state (green) and two views of the TS (light orange).

dimethyl 1*H*,1'*H*-[3,3'-bipyrrole]-4,4'-dicarboxylate (1d):

We modeled the barriers presented by the ester groups with **1d**. The minimum energy conformation is predicted to be at ~58° with the ester groups near planar to their respective heterocycles and adjacent to one another (the two methoxy oxygens are 3.2 Å apart). The carbonyl oxygen prefers to point away from the heterocyclic linkage (the 'flipped' geometry, with the carbonyl oxygen pointing 'in', is generally 1-2 kcal.mol^{-1} less favorable (data not shown)). The predicted TS energies are ~20 kcal.mol^{-1} and fall approximately 6 kcal.mol^{-1} lower than the syn TS for molecule **1** across the various model chemistries.

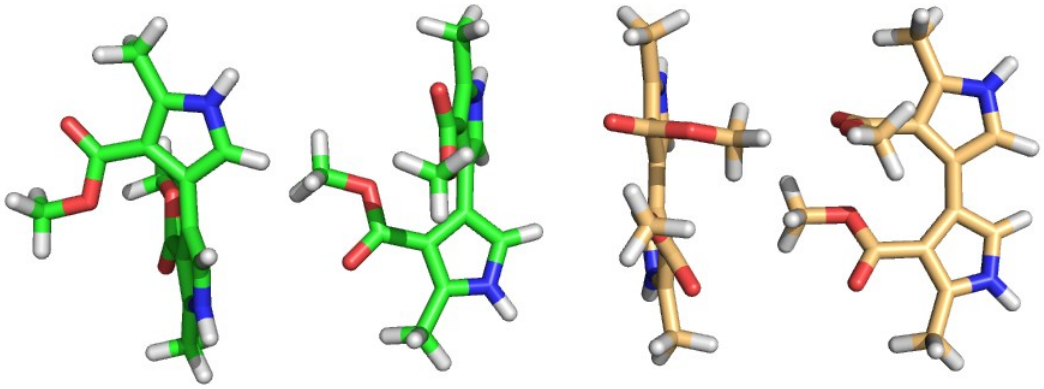

Figure S32: Two views of the **1d** predicted ground state (green) and two views of the TS (light orange).

Comparison with molecule 1:

The transition state for the isolated phenyl-ester crossing (molecule **1c**) is considerably less than that presented by the ester groups passaging each other (molecule **1d**), ~13 vs ~20 kcal.mol^{-1}, respectively. In contrast, molecule **1** is predicted to have a slight preference for the transition pathway in which the esters

cross. However, the molecule **1** transitions roughly correspond to additions of the isolated component barriers. For example, from the B3LYP energies, the *syn* barrier of molecule **1** is 26.1 kcal.mol^{-1} and the barriers for **1b** + **1d** = 10.9 + 21.0 = 31.9 kcal.mol^{-1}. For the *anti* barrier molecule **1** is 28.5 kcal.mol^{-1} and double the **1c** transition is 2*13.7 = 27.4 kcal.mol^{-1}. Although not exact, the additive effects do help explain the similar *syn* and *anti* barrier heights.

File tables of atom coordinates and absolute energies:

Conformation: Ground State (min):

Table S9: Cartesian coordinates (in Å) of the B3LYP/6-311G** optimized structure of the electronic ground state of molecule **1**. (Total energy: B3LYP/6-311G**: -1494.68221303 Hartrees, 0 imaginary frequencies)

Atom	x	y	z
N	-0.55505	-2.70428	-0.92979
N	-0.55494	2.70434	0.92970
C	0.10693	0.66733	0.31231
C	0.10690	-0.66732	-0.31235
C	-0.85658	-1.63745	-0.09527
C	0.58014	-2.47281	-1.64338
C	1.02264	-1.20028	-1.29088
C	1.02270	1.20028	1.29081
C	-0.85657	1.63745	0.09527
C	1.14379	-3.50339	-2.56597
C	0.58027	2.47285	1.64325
C	1.14393	3.50342	2.56585
C	-2.02120	1.69803	-0.79385
C	-3.20263	2.33854	-0.38521
C	-4.29710	2.43473	-1.23954
C	-4.23965	1.88302	-2.51694
C	-3.07518	1.23754	-2.93227
C	-1.97600	1.14934	-2.08556
C	-2.02117	-1.69802	0.79390
C	-1.97594	-1.14933	2.08561

C	-3.07509	-1.23752	2.93235
C	-4.23956	-1.88300	2.51706
C	-4.29706	-2.43473	1.23967
C	-3.20261	-2.33854	0.38530
C	2.23899	0.61382	1.85798
C	3.60002	-1.32554	2.02557
C	2.23895	-0.61384	-1.85804
C	3.59981	1.32565	-2.02586
O	3.03448	1.21470	2.55601
O	2.40311	-0.68693	1.52854
O	2.40287	0.68701	-1.52890
O	3.03458	-1.21482	-2.55583
C	3.66313	-2.71246	1.41714
C	3.66331	2.71226	-1.41675
H	-1.05065	-3.58174	-0.92099
H	-1.05063	3.58175	0.92102
H	1.58575	3.03475	3.44364
H	0.36659	-4.20522	-2.88261
H	0.36675	4.20531	2.88242
H	1.94295	-4.07379	-2.08129
H	1.58568	-3.03474	-3.44374
H	1.94315	4.07377	2.08121
H	3.55418	-1.35872	3.11746
H	4.46580	-0.71837	1.75191
H	-3.27806	2.73442	0.62214
H	-5.20064	2.92929	-0.90034
H	-5.09281	1.95404	-3.18200
H	-3.01756	0.81149	-3.92797
H	-1.06693	0.66900	-2.42380
H	-1.06686	-0.66898	2.42382
H	-3.01744	-0.81148	3.92805
H	-5.09272	-1.95402	3.18214
H	-5.20061	-2.92929	0.90050

H	-3.27806	-2.73443	-0.62204
H	3.55371	1.35941	-3.11773
H	4.46554	0.71817	-1.75272
H	2.78366	-3.29865	1.69287
H	4.55325	3.23471	-1.77847
H	4.55309	-3.23487	1.77885
H	3.71408	2.65542	-0.32749
H	3.71358	-2.65618	0.32783
H	2.78385	3.29872	-1.69191

Conformation: T.S.-I (~ 180 degrees):

Table S10: Cartesian coordinates (in Å) of the B3LYP/6-311G**: optimized structure of the electronic transition state-I of molecule **1**. (Total energy B3LYP/6-311G**: -1494.63707021 Hartrees, 1 imaginary frequency)

Atom	x	y	z
N	-0.67790	-2.73003	0.13939
N	0.47924	3.01002	-0.65155
C	-0.12875	0.88816	-0.24014
C	-0.09517	-0.58652	-0.18785
C	-1.18470	-1.46442	-0.10745
C	0.67923	-2.74269	0.12817
C	1.08914	-1.43679	-0.10955
C	-1.30546	1.74473	-0.37060
C	0.96767	1.75370	-0.33675
C	1.43092	-4.02925	0.27089
C	-0.87983	3.03280	-0.66738
C	-1.62495	4.30486	-0.90869
C	2.39079	1.71048	0.04346
C	3.36552	2.34418	-0.74263
C	4.68198	2.44153	-0.30491
C	5.05511	1.89937	0.92429
C	4.09739	1.26101	1.71067

C	2.77653	1.17424	1.28022
C	-2.61987	-1.42804	-0.44239
C	-3.54564	-2.16865	0.31326
C	-4.87127	-2.28783	-0.09370
C	-5.30534	-1.65966	-1.25958
C	-4.39899	-0.91971	-2.01579
C	-3.06924	-0.81452	-1.62100
C	-2.68607	1.60069	0.13379
C	-4.00805	0.87146	1.96607
C	2.43928	-1.19874	-0.65210
C	4.72497	-1.83967	-0.52951
O	-3.66638	2.13443	-0.34207
O	-2.72265	0.92586	1.30706
O	3.38874	-1.90559	0.01895
O	2.69464	-0.54224	-1.63433
C	-3.78828	0.26532	3.33785
C	5.61858	-2.70328	0.33852
H	-1.25178	-3.55828	0.12818
H	1.06272	3.83091	-0.68456
H	-2.67851	4.17645	-0.67193
H	0.73515	-4.86258	0.40159
H	-1.56086	4.59607	-1.96304
H	2.10319	-4.00357	1.12989
H	2.04372	-4.23705	-0.60959
H	-1.21659	5.12658	-0.31057
H	-4.69117	0.27479	1.35855
H	-4.41323	1.88368	2.02870
H	3.09372	2.72729	-1.71977
H	5.42125	2.92954	-0.93063
H	6.08102	1.97621	1.26683
H	4.37449	0.84254	2.67198
H	2.03062	0.70057	1.90703
H	-3.22497	-2.63856	1.23732

H	-5.56780	-2.86318	0.50664
H	-6.33888	-1.74576	-1.57488
H	-4.72480	-0.42635	-2.92418
H	-2.36611	-0.26260	-2.23243
H	5.04822	-0.79705	-0.53350
H	4.70264	-2.18521	-1.56618
H	-3.38272	-0.74561	3.26034
H	6.64660	-2.66398	-0.03194
H	-4.73739	0.21543	3.87880
H	5.29189	-3.74585	0.32886
H	-3.09011	0.86970	3.92142
H	5.61269	-2.35032	1.37219

Conformation: T.S.-II (~ 0 degrees):

Table S11: Cartesian coordinates (in Å) of the B3LYP/6-311G** optimized structure of the electronic transition state-II of molecule **1**. (Total energy: B3LYP/6-311G**: -1494. 64052083 Hartrees, 1 imaginary frequency)

Atom	x	y	z
N	-0.50209	-2.87375	0.33581
N	-0.50208	2.87378	-0.33575
C	0.13346	0.74048	-0.01295
C	0.13345	-0.74046	0.01295
C	-0.97614	-1.59803	0.07440
C	0.85533	-2.91579	0.33868
C	1.29611	-1.62109	0.10502
C	1.29611	1.62111	-0.10500
C	-0.97613	1.59805	-0.07437
C	1.58251	-4.20744	0.52631
C	0.85534	2.91581	-0.33861
C	1.58251	4.20747	-0.52626
C	-2.39897	1.54662	0.31084

C	-2.78312	0.99341	1.54070
C	-4.09214	1.10979	1.99385
C	-5.04502	1.78844	1.23520
C	-4.67778	2.34409	0.01244
C	-3.36903	2.22268	-0.44613
C	-2.39897	-1.54662	-0.31083
C	-3.36904	-2.22269	0.44612
C	-4.67777	-2.34412	-0.01247
C	-5.04500	-1.78846	-1.23523
C	-4.09212	-1.10979	-1.99386
C	-2.78311	-0.99340	-1.54069
C	2.69414	1.45546	0.33209
C	4.10440	0.50395	2.00715
C	2.69411	-1.45548	-0.33212
C	4.10436	-0.50398	-2.00720
O	3.64587	2.07085	-0.10828
O	2.79425	0.63471	1.40131
O	2.79422	-0.63470	-1.40132
O	3.64583	-2.07092	0.10820
C	3.96055	-0.43852	3.18419
C	3.96050	0.43854	-3.18421
H	-1.09428	-3.68867	0.31140
H	-1.09428	3.68869	-0.31131
H	2.59824	4.13430	-0.14427
H	1.06301	-5.02880	0.02220
H	1.06333	5.02874	-0.02167
H	1.65859	-4.46135	1.58937
H	2.59806	-4.13446	0.14380
H	1.65805	4.46167	-1.58929
H	4.44707	1.49725	2.30685
H	4.80101	0.11034	1.26604
H	-2.03892	0.49040	2.14661
H	-4.36719	0.68063	2.95102

H	-6.06353	1.88226	1.59436
H	-5.41237	2.86626	-0.59071
H	-3.09768	2.64016	-1.41025
H	-3.09769	-2.64018	1.41024
H	-5.41236	-2.86630	0.59066
H	-6.06351	-1.88229	-1.59441
H	-4.36716	-0.68062	-2.95103
H	-2.03891	-0.49038	-2.14659
H	4.44697	-1.49728	-2.30694
H	4.80102	-0.11042	-1.26610
H	3.22577	-0.06105	3.89920
H	4.92167	0.53907	-3.69612
H	4.92173	-0.53907	3.69608
H	3.64710	1.42469	-2.83899
H	3.64710	-1.42468	2.83902
H	3.22569	0.06111	-3.89920

Section III: Analytical data for compound 2

III.a) ECD Spectra

Electronic Circular Dichroism (ECD) spectra (ethanol, 2.20 mM) were recorded at 293 K. The spectral data were obtained is represented below in figure S33. Like compound **1**, *R*-(+)-**2** showed positive CD spectra.

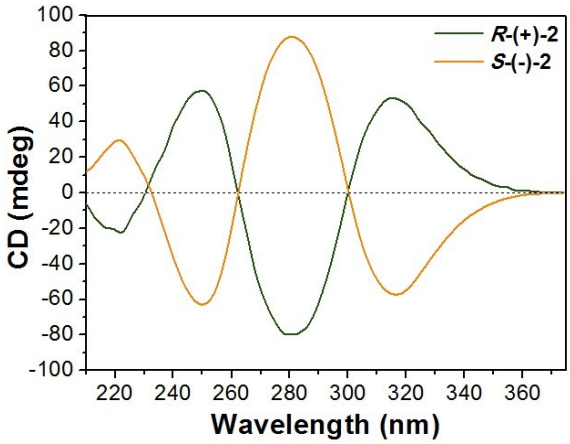

Figure S33: ECD-spectra of two atropisomers of **2**

III.b) HPLC profiles at different time intervals at 353 K

Same experimental method was employed as in **Section II.c**. Individual samples were subjected to chiral HPLC analysis by using following condition:

Column: Chiral CEL OD-H (4.6 mm x 250.0 mm x 5.0 µm)

Solvent: 0.30 % diethyl amine in hexane : ethanol (90 : 10)

Flow rate: 1.0 mL/min

Mode: Binary gradient

Column oven: 298 K

Injected volume: 40.0 µL

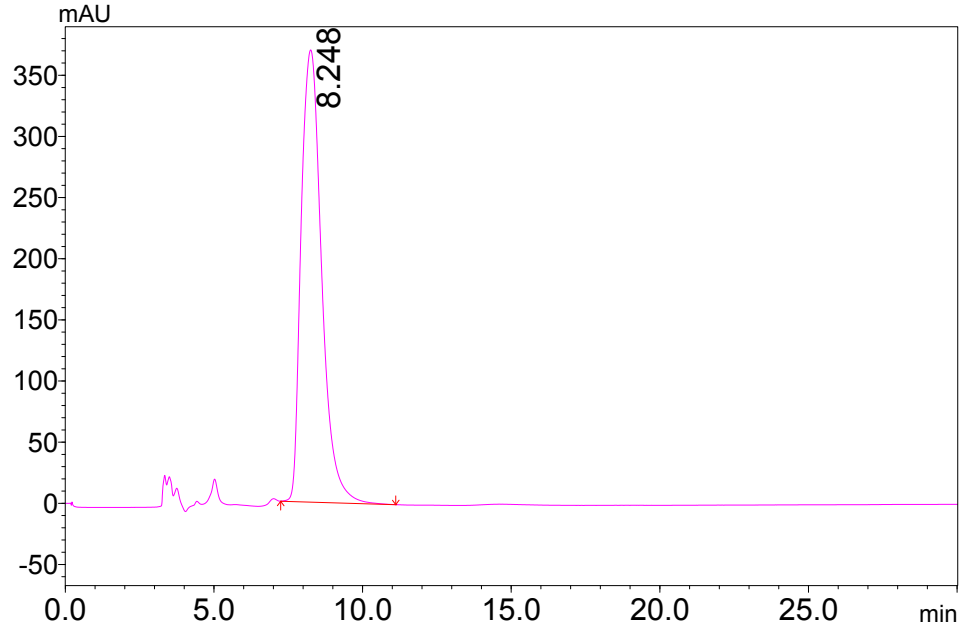

PDA Ch1 254nm 4nm

Peak#	Ret. Time	Area	Height	Area %	Height %
1	8.248	17724346	369760	100.000	100.000
Total		17724346	369760	100.000	100.000

Figure S34: Chiral HPLC profile of (*R*)-**2** at 0 min (before placing incubation at 353 K)

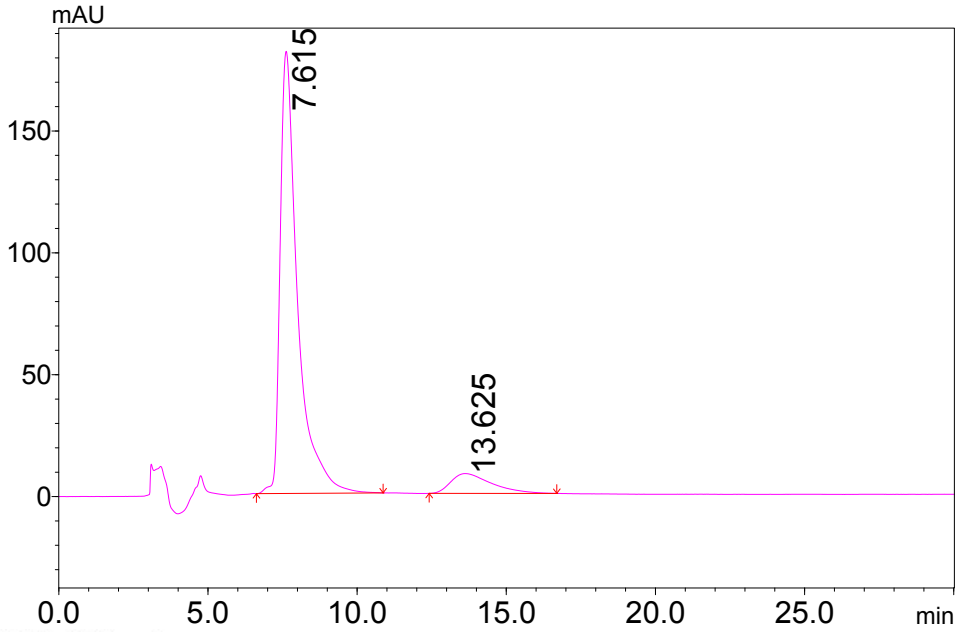

PDA Ch1 254nm 4nm

Peak#	Ret. Time	Area	Height	Area %	Height %
1	7.615	7379074	181417	90.547	95.715
2	13.625	770397	8121	9.453	4.285
Total		8149471	189538	100.000	100.000

Figure S35: Chiral HPLC profile of (*R*)-**2** at 10 min (353 K)

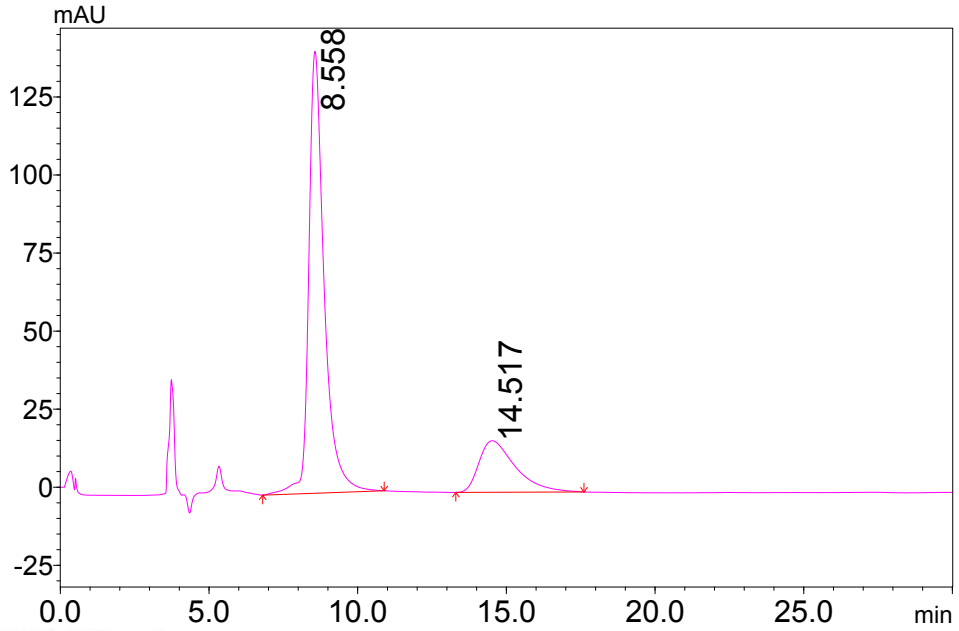

PDA Ch1 254nm 4nm

Peak#	Ret. Time	Area	Height	Area %	Height %
1	8.558	5102622	141537	78.448	89.552
2	14.517	1401812	16512	21.552	10.448
Total		6504434	158049	100.000	100.000

Figure S36: Chiral HPLC profile of (*R*)-**2** at 20 min (353 K)

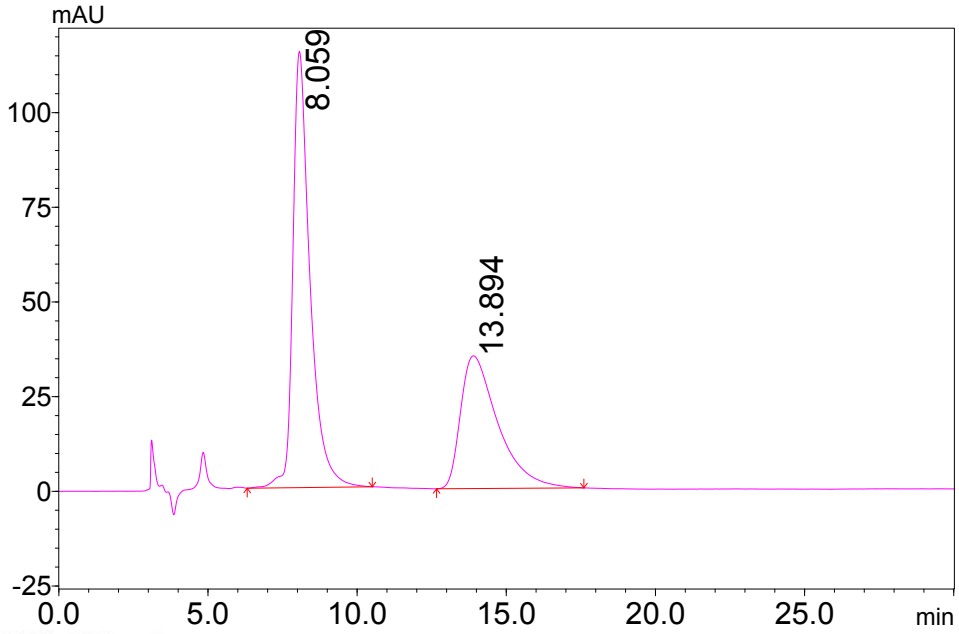

PDA Ch1 254nm 4nm

Peak#	Ret. Time	Area	Height	Area %	Height %
1	8.059	4623408	115171	60.271	76.668
2	13.894	3047609	35050	39.729	23.332
Total		7671017	150220	100.000	100.000

Figure S37: Chiral HPLC profile of (*R*)-**2** at 40 min (353 K)

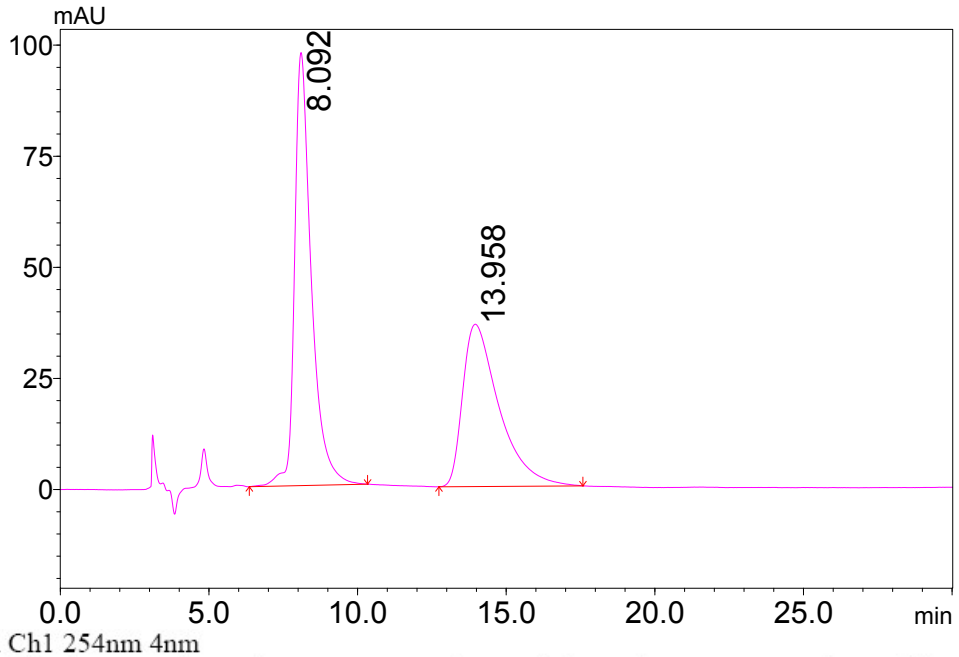

PDA Ch1 254nm 4nm

Peak#	Ret. Time	Area	Height	Area %	Height %
1	8.092	3833435	97446	55.168	72.733
2	13.958	3115282	36531	44.832	27.267
Total		6948716	133977	100.000	100.000

Figure S38: Chiral HPLC profile of (*R*)-**2** at 60 min (353 K)

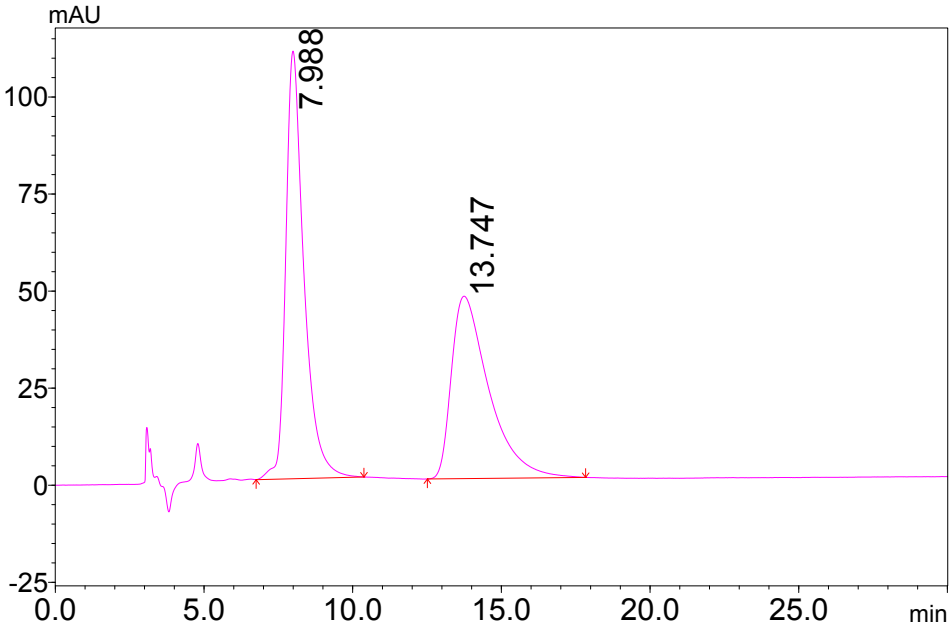

PDA Ch1 254nm 4nm

Peak#	Ret. Time	Area	Height	Area %	Height %
1	7.988	4688999	110156	53.255	70.102
2	13.747	4115833	46982	46.745	29.898
Total		8804832	157138	100.000	100.000

Figure S39: Chiral HPLC profile of (*R*)-**2** at 80 min (353 K)

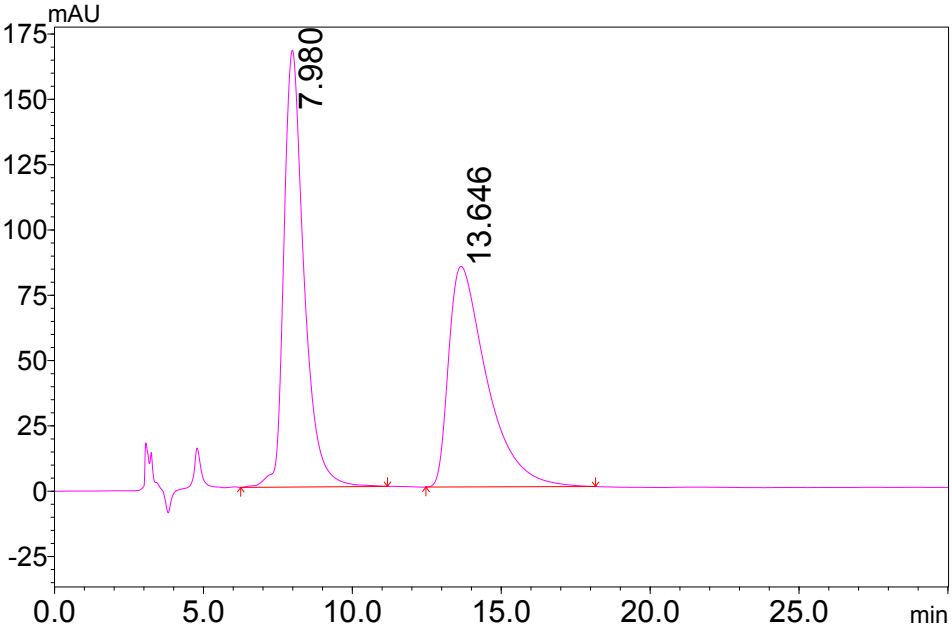

PDA Ch1 254nm 4nm

Peak#	Ret. Time	Area	Height	Area %	Height %
1	7.980	7897242	167169	51.210	66.436
2	13.646	7524109	84454	48.790	33.564
Total		15421351	251623	100.000	100.000

Figure S40: Chiral HPLC profile of (*R*)-**2** at 100 min (353 K)

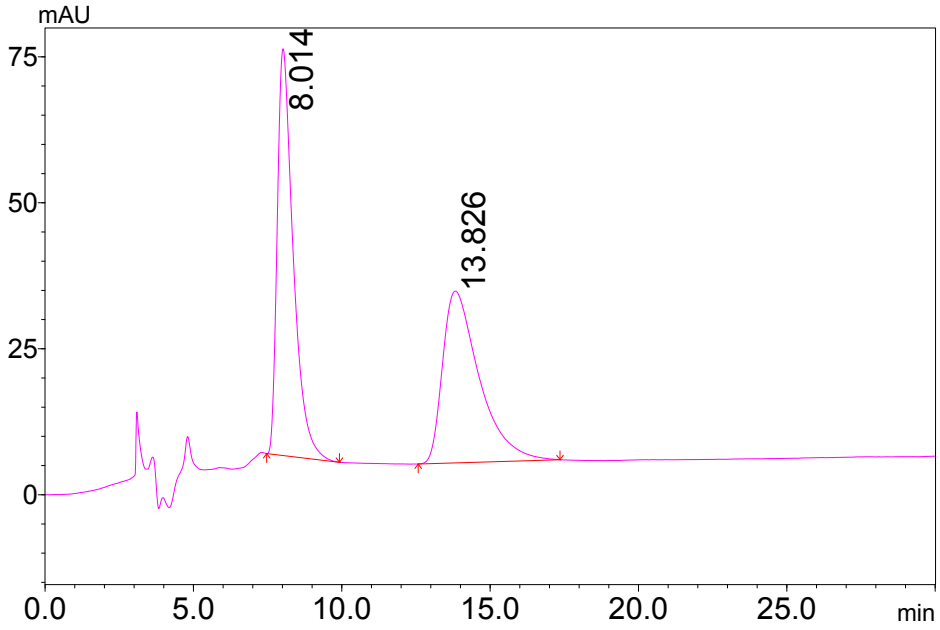

PDA Ch1 254nm 4nm

Peak#	Ret. Time	Area	Height	Area %	Height %
1	8.014	2607376	69660	50.729	70.303
2	13.826	2532391	29426	49.271	29.697
Total		5139767	99085	100.000	100.000

Figure S41: Chiral HPLC profile of (*R*)-**2** at 120 min (353 K)

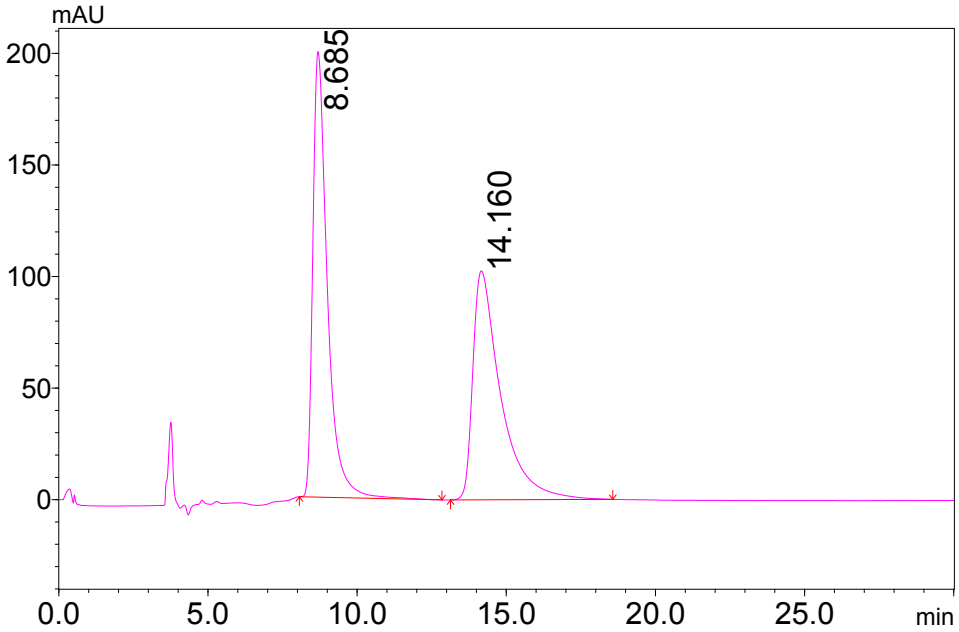

PDA Ch1 254nm 4nm

Peak#	Ret. Time	Area	Height	Area %	Height %
1	8.685	6774342	199630	50.350	66.042
2	14.160	6680092	102646	49.650	33.958
Total		13454434	302276	100.000	100.000

Figure S42: Chiral HPLC profile of (*R*)-**2** at 140 min (353 K)

III.c) Determination of kinetic and thermodynamical parameters from HPLC analysis

Time dependent chiral HPLC analysis was performed on enantiopure (*R*)-**2** following the experimental protocol mentioned in **section III.b**. The decrease of enantiomeric excess (*ee*) with time at 353 K incubation temperature is shown in figure S43 and summarized in table S12. Decrease of enantiopurity (*ee* %) of (*R*)-**2** at 353 K experimental temperature was plotted as a function of variable time regime. From the exponential decay curve (shown in figure S43), energy to racemization and other parameters were determined from the decay constant (t_1) as 30.653 min, following equations 1-5 described in **section II.b**.

Table S12: Decrease of enantiomeric excess (*ee* %) with time during incubation of (*R*)-**2** at 353 K.

Time (min)	0	10	20	40	60	80	100	120	140	160
ee (%)	>99.0	81.09	56.89	20.54	10.33	6.51	2.42	1.46	0.70	[n.r.][a]

[a] [n.r.] = not required (molecule **2** was racemized at 140 min)

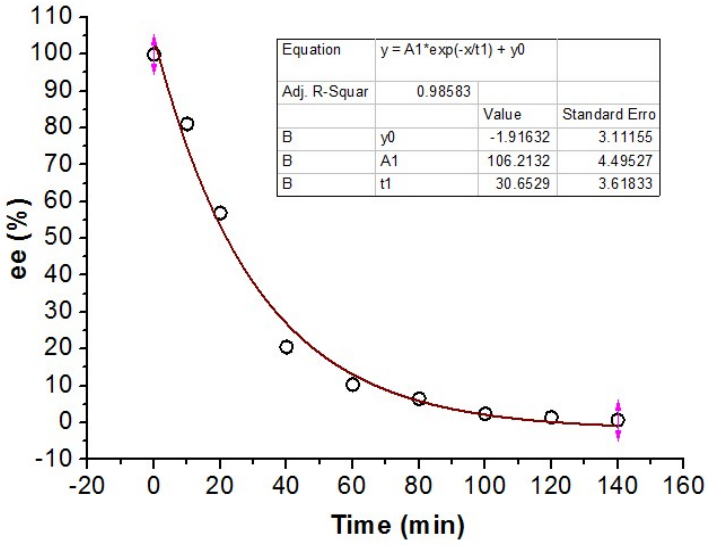

Figure S43: Plot of *ee* (%) of (*R*)-bipyrrole (**2**) as a function of time (min.) at 353 K for the determination of its conformational stability by chiral HPLC.
Regression value of first order decay = 0.98583.

Section IV: Analytical data for compound 3

IV.a) ECD Spectra

Electronic Circular Dichroism (ECD) spectra (ethanol, 2.20 mM) were recorded at 293 K. The spectral data were obtained is represented below in figure S44. Like compound **1**, *R*-(+)-**3** also showed positive CD spectra.

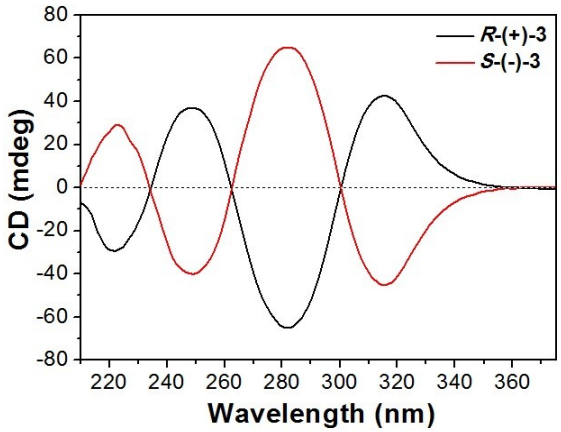

Figure S44: ECD-spectra of two atropisomers of **3**

IV.b) HPLC profiles at different time intervals at 353 K

Same experimental method was employed as in **section II.c**. Individual samples were subjected to chiral HPLC analysis by using following condition:

Column: Chiral CEL OD-H (4.6 mm x 250.0 mm x 5.0 µm)

Solvent: 0.30 % diethyl amine in hexane : ethanol (90 : 10)

Flow rate: 1.0 mL/min

Mode: Binary gradient

Column oven: 298 K

Injected volume: 40.0 µL

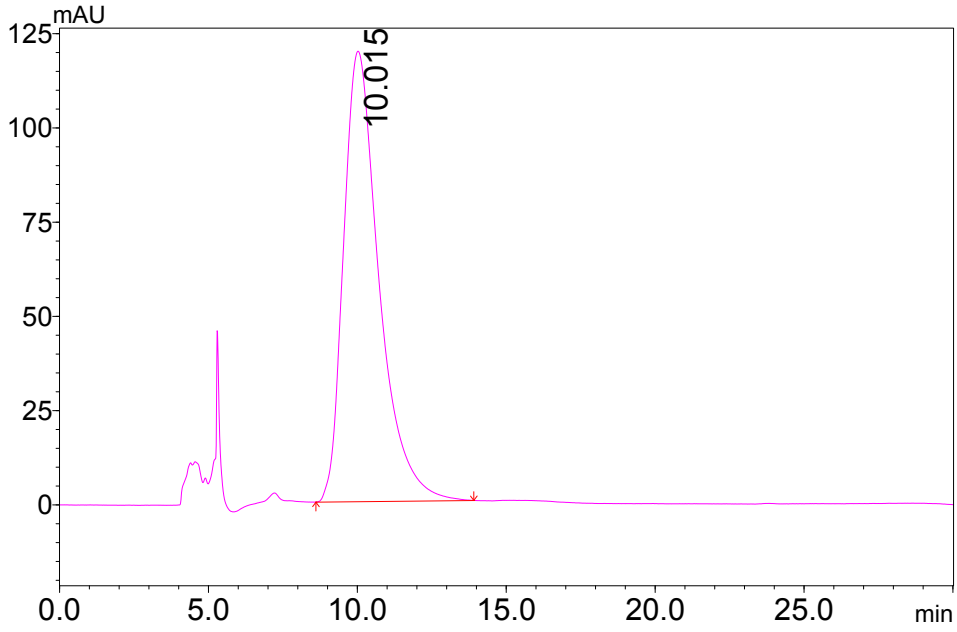

PDA Ch1 254nm 4nm

Peak#	Ret. Time	Area	Height	Area %	Height %
1	10.015	9896397	119478	100.000	100.000
Total		9896397	119478	100.000	100.000

Figure S45: Chiral HPLC profile of (*R*)-**3** at 0 min (before placing incubation at 353 K)

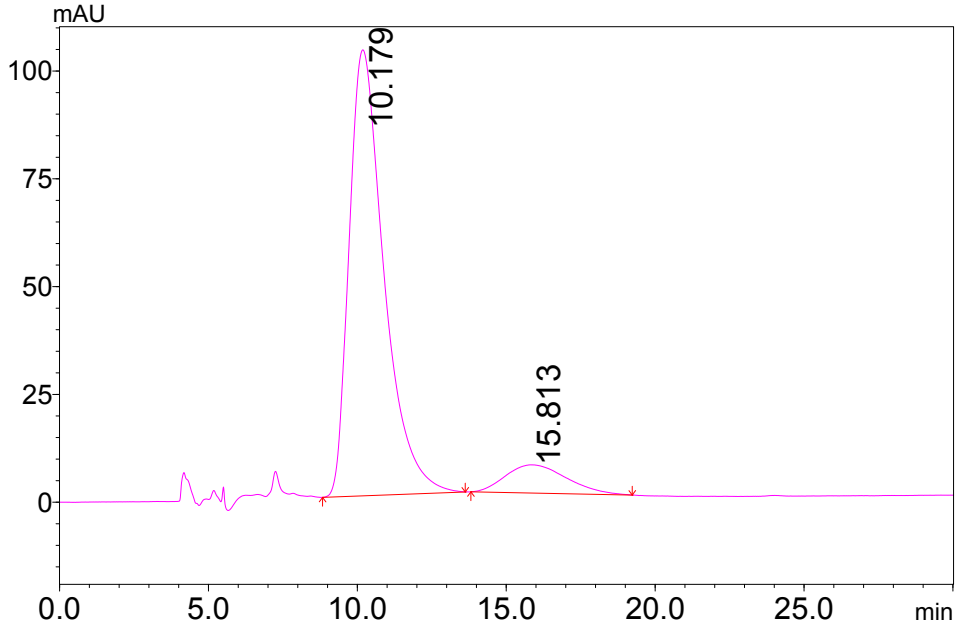

PDA Ch1 254nm 4nm

Peak#	Ret. Time	Area	Height	Area %	Height %
1	10.179	8414788	103444	89.992	94.057
2	15.813	935779	6536	10.008	5.943
Total		9350566	109980	100.000	100.000

Figure S46: Chiral HPLC profile of (*R*)-**3** at 10 min (353 K)

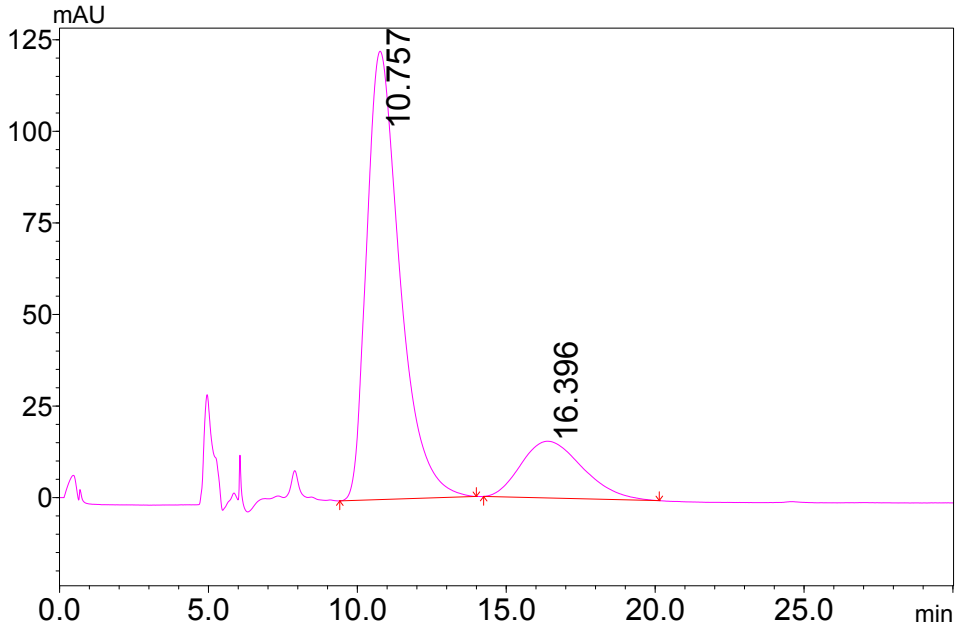

PDA Ch1 254nm 4nm

Peak#	Ret. Time	Area	Height	Area %	Height %
1	10.757	9522342	122401	81.022	88.765
2	16.396	2230474	15492	18.978	11.235
Total		11752815	137892	100.000	100.000

Figure S47: Chiral HPLC profile of (*R*)-**3** at 20 min (353 K)

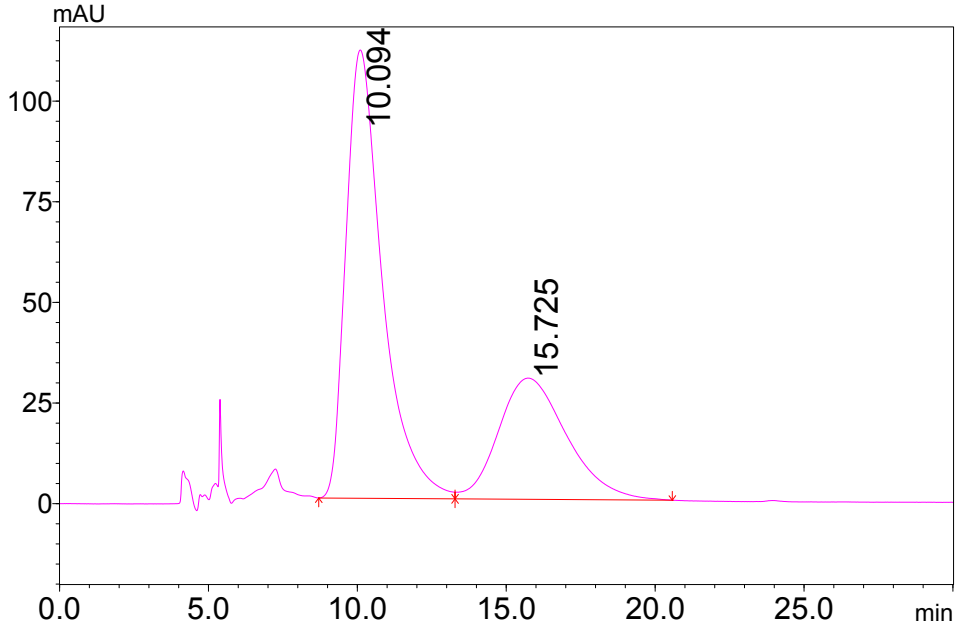

PDA Ch1 254nm 4nm

Peak#	Ret. Time	Area	Height	Area %	Height %
1	10.094	9534319	111360	66.456	78.715
2	15.725	4812523	30112	33.544	21.285
Total		14346842	141472	100.000	100.000

Figure S48: Chiral HPLC profile of (*R*)-**3** at 40 min (353 K)

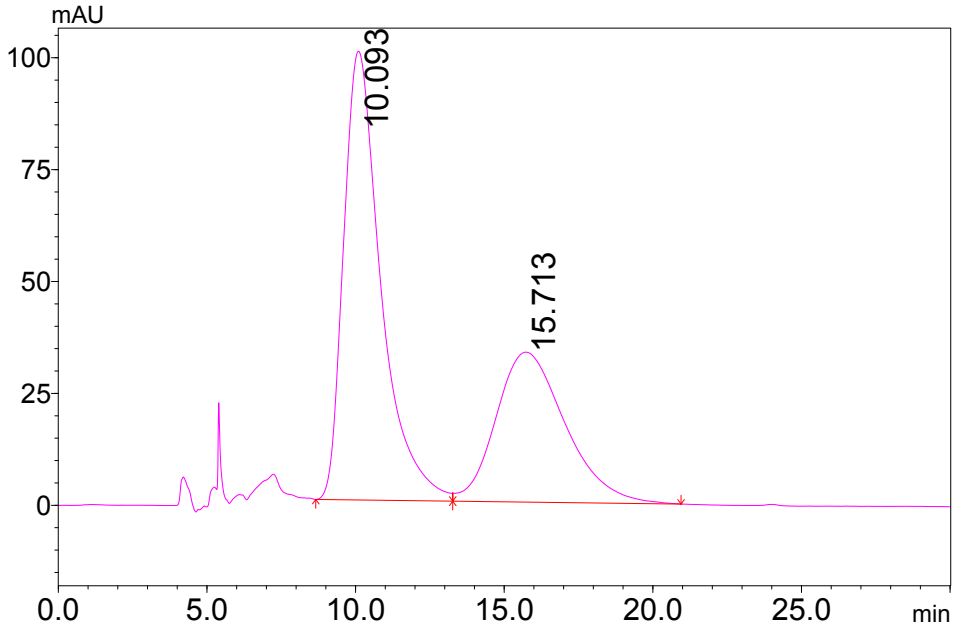

PDA Ch1 254nm 4nm

Peak#	Ret. Time	Area	Height	Area %	Height %
1	10.093	8771823	100257	61.747	74.953
2	15.713	5434178	33503	38.253	25.047
Total		14206001	133760	100.000	100.000

Figure S49: Chiral HPLC profile of (*R*)-**3** at 60 min (353 K)

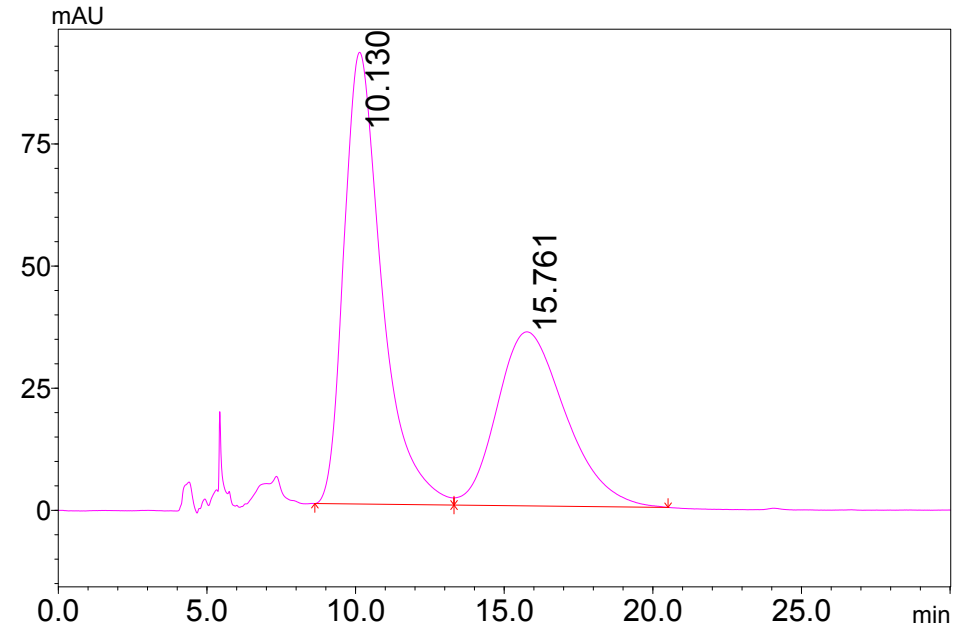

PDA Ch1 254nm 4nm

Peak#	Ret. Time	Area	Height	Area %	Height %
1	10.130	8237767	92477	58.970	72.179
2	15.761	5731542	35645	41.030	27.821
Total		13969310	128122	100.000	100.000

Figure S50: Chiral HPLC profile of (*R*)-**3** at 80 min (353 K)

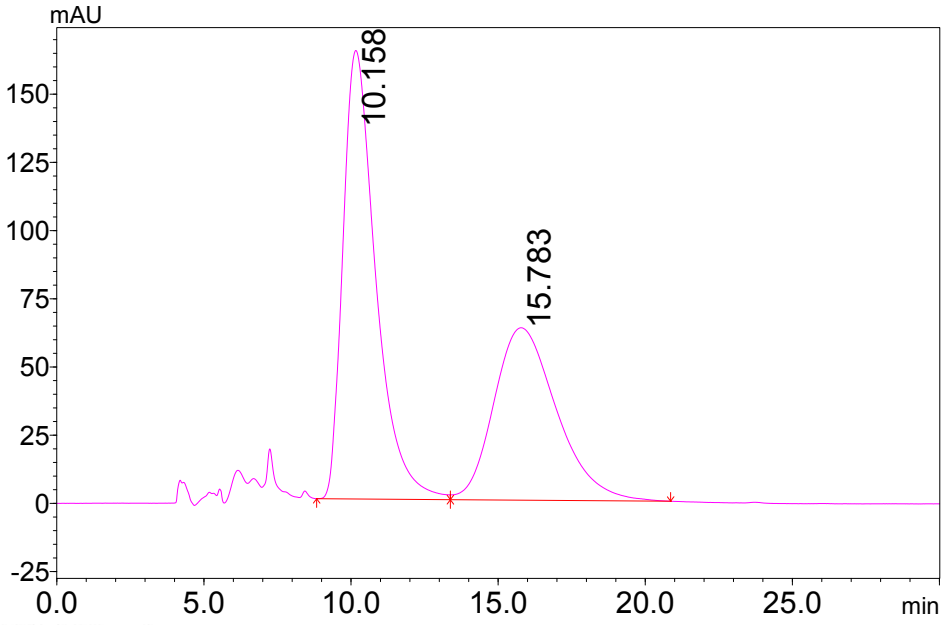

PDA Ch1 254nm 4nm

Peak#	Ret. Time	Area	Height	Area %	Height %
1	10.158	12797474	164427	57.685	72.231
2	15.783	9387742	63212	42.315	27.769
Total		22185215	227639	100.000	100.000

Figure S51: Chiral HPLC profile of (*R*)-**3** at 100 min (353 K)

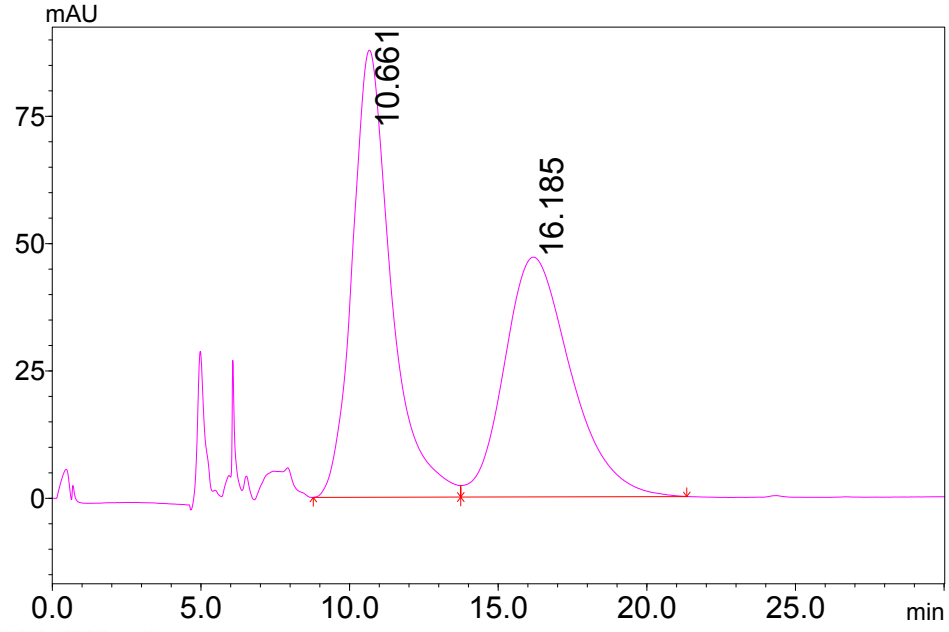

PDA Ch1 254nm 4nm

Peak#	Ret. Time	Area	Height	Area %	Height %
1	10.661	8006309	87784	52.187	65.091
2	16.185	7335286	47080	47.813	34.909
Total		15341595	134863	100.000	100.000

Figure S52: Chiral HPLC profile of (*R*)-**3** at 120 min (353 K)

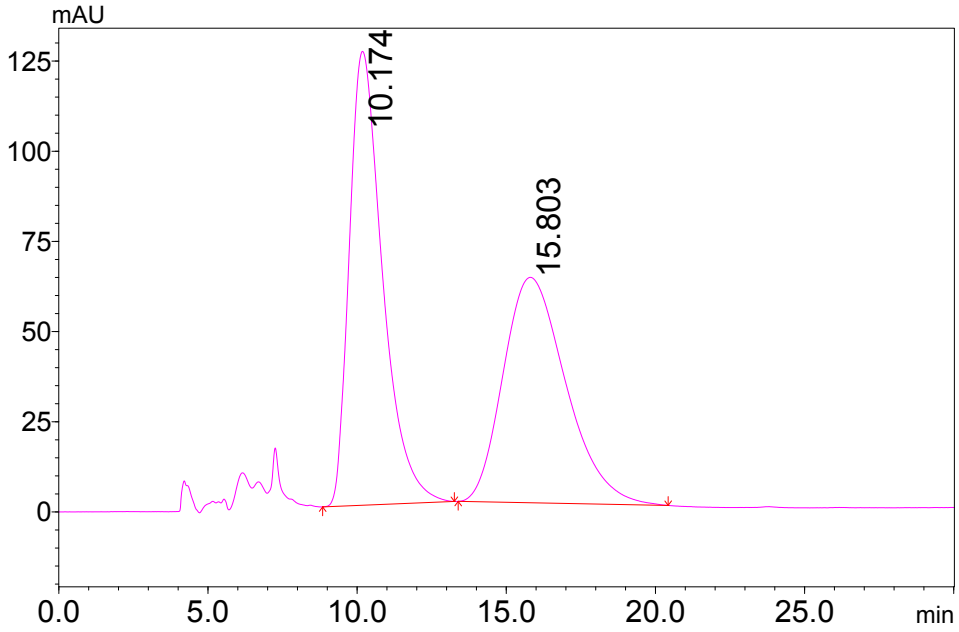

PDA Ch1 254nm 4nm

Peak#	Ret. Time	Area	Height	Area %	Height %
1	10.174	9759616	125822	51.670	66.815
2	15.803	9128723	62491	48.330	33.185
Total		18888339	188313	100.000	100.000

Figure S53: Chiral HPLC profile of (*R*)-**3** at 140 min (353 K)

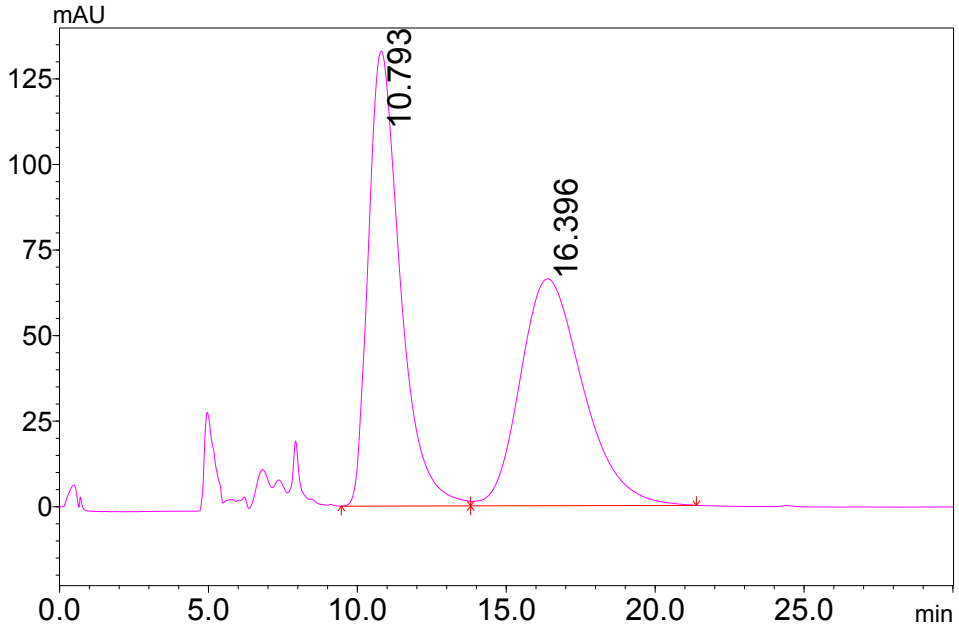

PDA Ch1 254nm 4nm

Peak#	Ret. Time	Area	Height	Area %	Height %
1	10.793	9944111	132944	50.568	66.729
2	16.396	9720633	66287	49.432	33.271
Total		19664744	199231	100.000	100.000

Figure S54: Chiral HPLC profile of (*R*)-**3** at 160 min (353 K)

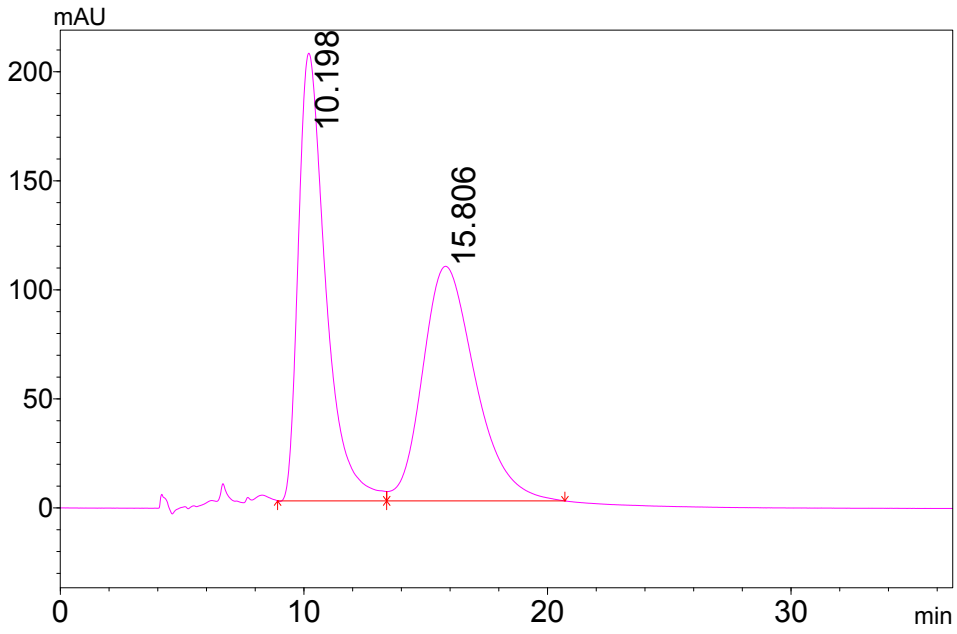

PDA Ch1 254nm 4nm

Peak#	Ret. Time	Area	Height	Area %	Height %
1	10.198	16061245	205257	49.757	65.614
2	15.806	16217814	107569	50.243	34.386
Total		32279059	312826	100.000	100.000

Figure S55: Chiral HPLC profile of (*R*)-**3** at 170 min (353 K)

IV.c) Determination of kinetic and thermodynamical parameters from HPLC analysis

Time dependent chiral HPLC analysis was performed on enantiopure (*R*)-**3** following the experimental protocol mentioned in **section IV.b**. The decrease of enantiomeric excess (*ee*) with time at 353 K incubation temperature is shown in figure S56 and summarized in table S13. Decrease of enantiopurity (*ee* %) of (*R*)-**3** at 353 K experimental temperature was plotted as a function of variable time regime. From the exponential decay curve (shown in figure S56), energy to racemization and other parameters were determined from the decay constant (t_1) as 41.0510 min, following equations 1-5 described in **section II.b**.

Table S13: Decrease of enantiomeric excess (*ee* %) with time during incubation of (*R*)-**3** at 353 K.

Time (min)	0	10	20	40	60	80	100	120	140	160	170
ee (%)	>99.0	79.98	62.04	32.91	23.49	17.94	15.37	4.37	3.34	1.13	0.49

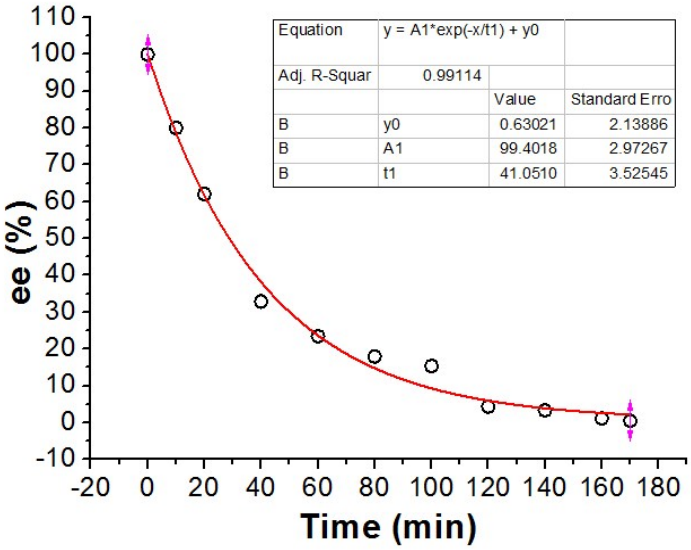

Figure S56: Plot of *ee* (%) of (*R*)-bipyrrole (**3**) as a function of time (min.) at 353 K for the determination of its conformational stability by chiral HPLC.
Regression value of first order decay = 0.99114.

Section V: Combined plot of enantiomeric excess vs time of compounds 1-3

The decrease of enantiomeric excess (*ee*) of *R*)-(+)-bipyrroles (**1-3**) with time at 353 K incubation temperature was studied by chiral HPLC analysis. A combined plot of *ee* (%) of (*R*)-(+)-bipyrroles (**1-3**) as a function of time (min.) at 353 K is shown in figure S57 as a comparison study.

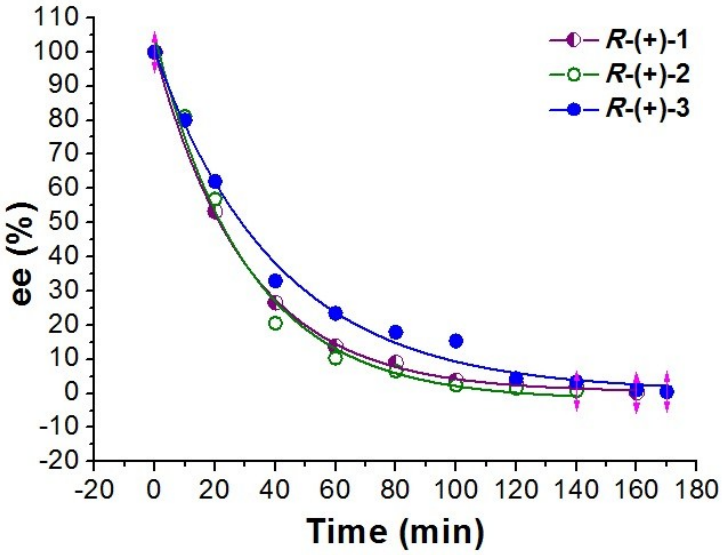

Figure S57: Combined plot of *ee* (%) of (*R*)-(+)-bipyrroles (**1-3**) as a function of time (min.) at 353 K as a comparison study by chiral HPLC

Section VI: ^{1}H NMR and ^{13}C NMR Spectra of 1-3

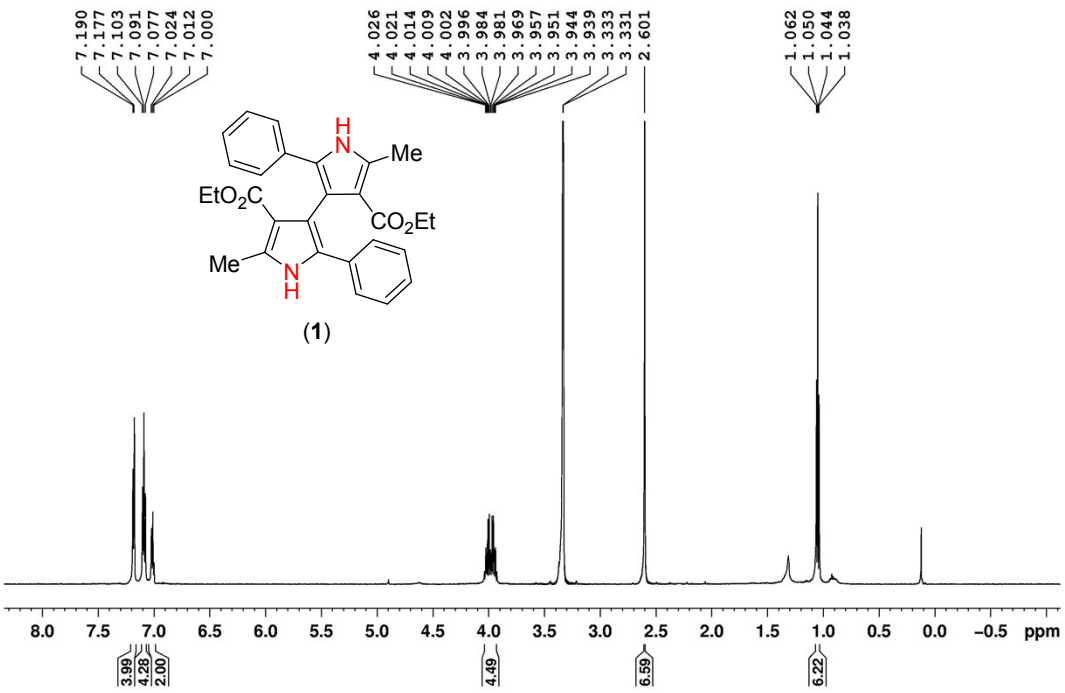

Figure S58: ^{1}H NMR spectrum of **1** in CD_3OD at 600 MHz

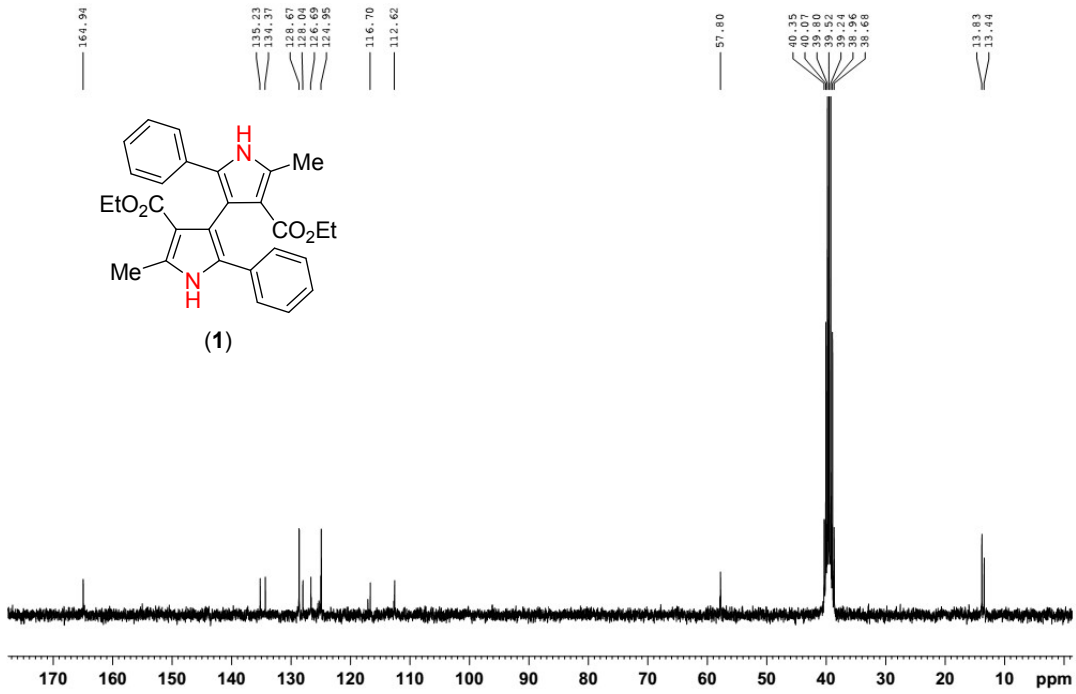

Figure S59: ^{13}C NMR spectrum of **1** in DMSO-d_6 at 300 MHz

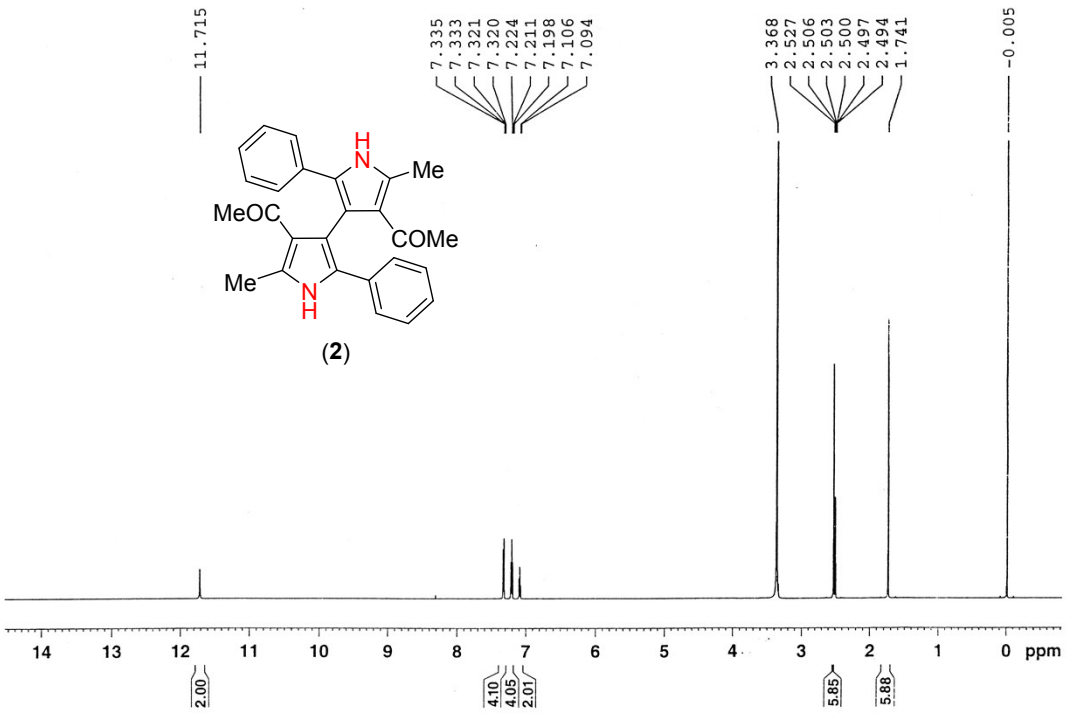

Figure S60: ^{1}H NMR spectrum of **2** in DMSO-d_6 at 600 MHz

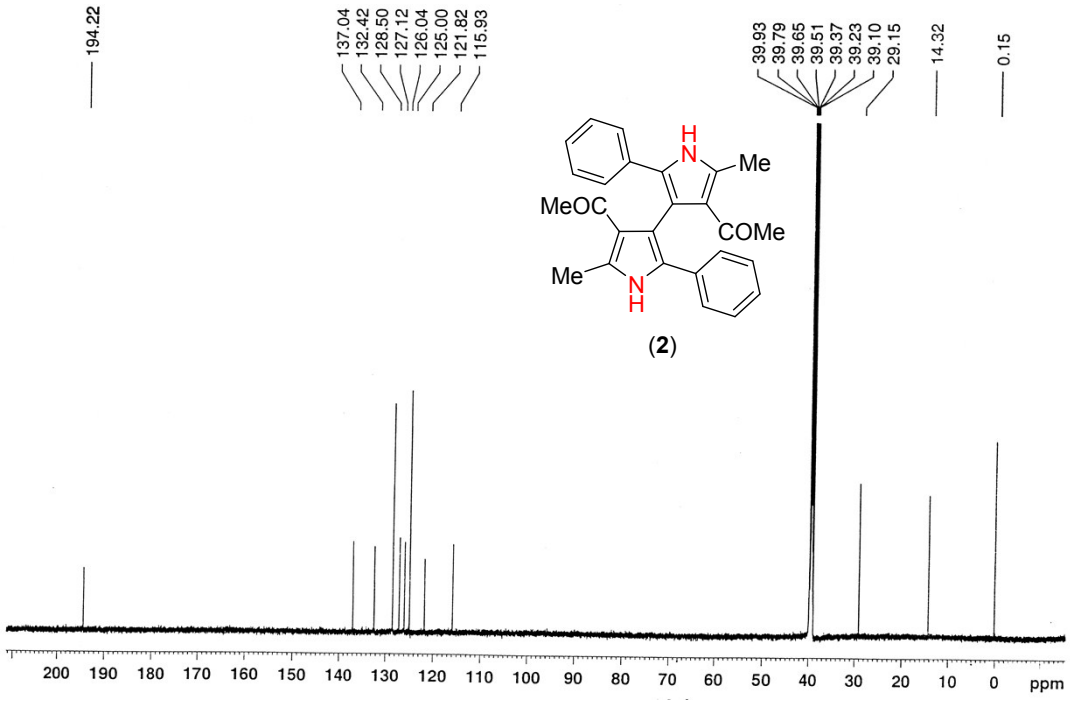

Figure S61: ^{13}C NMR spectrum of **2** in DMSO-d_6 at 600 MHz

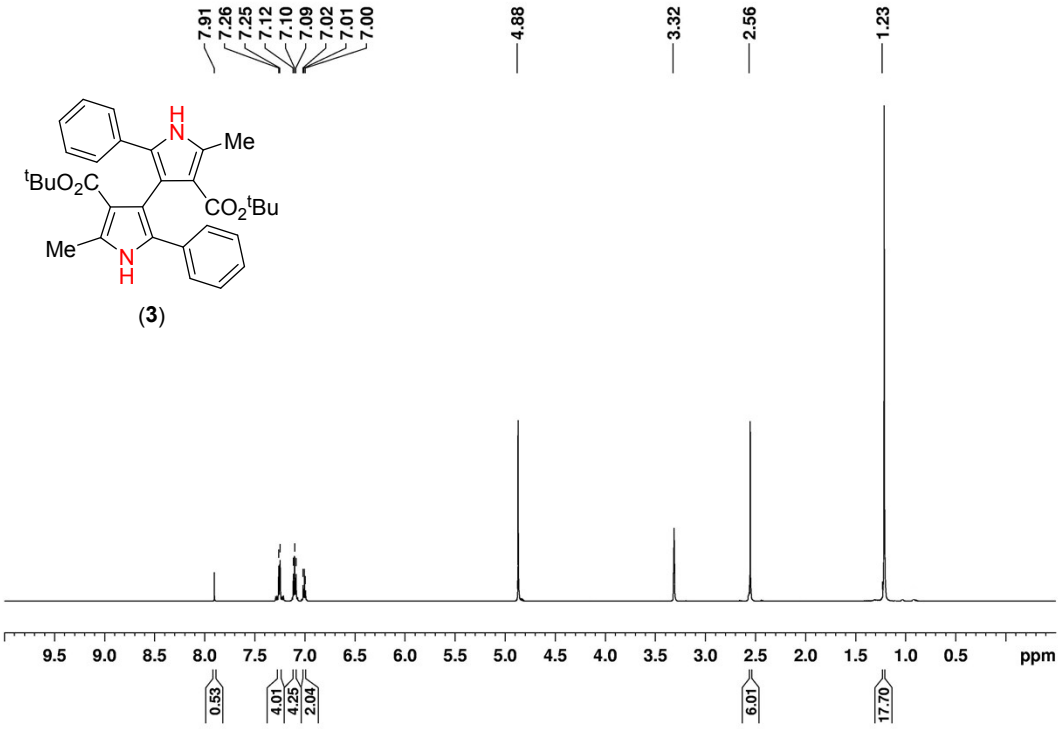

Figure S62: ^{1}H NMR spectrum of **3** in CD_3OD at 600 MHz

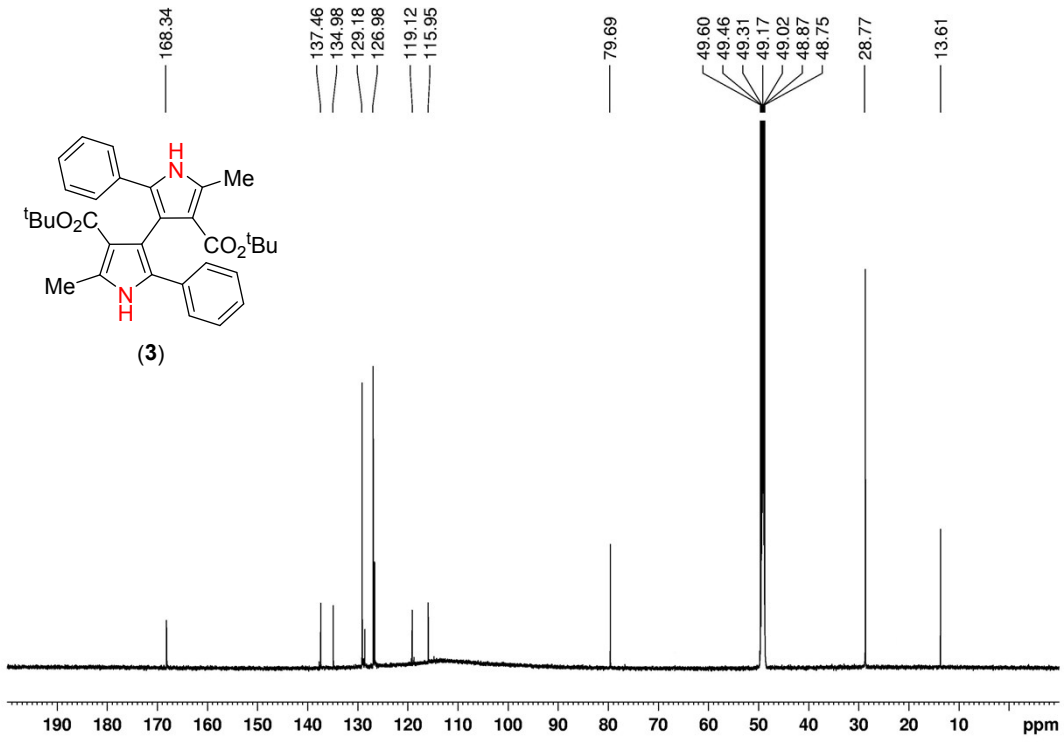

Figure S63: ^{13}C NMR spectrum of **3** in CD_3OD at 600 MHz

Section VII: References

1. S. Dey, C. Pal, D. Nandi, V. S. Giri, M. Zaidlewicz, M. Krzeminski, L. Smentek, B. A. Jr. Hess, J. Gawronski, M. Kwit, N. J. Babu, A. Nangia, P. Jaisankar, *Org. Lett*., 2008, **10**, 1373.

2. (a) C. Wolf, *Dynamic Stereochemistry of Chiral Compounds. Principles and Applications*; RSC Publishing: Cambridge, U.K., 2008. (b) E. Kumarasamy, R. Raghunathan, M. P. Sibi, J. Sivaguru, *Chem. Rev.,* 2015, **115**, 20, 11239. (c) C. Wolf, G. E. Tumambac, *J. Phys. Chem. A*., 2003, **107**, 815.

3. R. A. Jones, G. P. Bean, The Chemistry of Pyrroles: Organic Chemistry: A Series of Monographs, Academic Press: New York, 1977, **34**, 209.

4. M. S. Betson, J. Clayden, C. P. Worrall, S. Peace, *Angew. Chem., Int. Ed.,* 2006, **45**, 5803.